RESEARCH
**REPORT 313**
NOVEMBER 1966

AD 644258

# LOW FREQUENCY SHALLOW WATER
# INTERNAL WAVES AT PANAMA CITY, FLORIDA

Subproject ZF 011 01 01, Task 11275-11

GEORGE B. DOWLING

**UNITED STATES NAVY MINE DEFENSE LABORATORY**
P A N A M A   C I T Y ,   F L O R I D A

## ABSTRACT

Internal waves were investigated in water depths of 60 to 100 feet (18 to 30 m) during the time of strong summer stratification, and in the presence of well-developed internal tides.

Cross-spectral analyses indicate that free, low-frequency, internal waves were present during the three-day survey, although the data were contaminated by incoherent noise due to turbulence. The data were found to satisfy the characteristic equation from internal wave theory. Other evidence is the significant coherence between thermal fluctuations at mid-depth and current direction fluctuations at the bottom, implying shallow water internal waves.

The assumption that the density varies as the hyperbolic tangent with depth agrees well with the observed average density distribution and permits obtaining from internal wave theory an analytical expression for variation of internal wave phase velocity with depth at any given frequency. Shallow-water internal waves in such a density profile are dissipated by divergence of wave energy into the upper and lower turbulently mixed layers, accounting in part for the observed low coherence of internal waves.

Power spectra of observed isotherm fluctuations have a form consistent with the theory of anisotropic turbulence. Observed spectra result from superposition of two classes of spectra, one (weaker) due to internal waves, and one (stronger) due to turbulence.

Theory and experimental data support (1) the concept of interaction of internal waves, shear flows, and turbulence, (2) the conjecture that these interactions determine the equilibrium density profile, (3) the conclusion that internal waves, at least in shallow water, are accompanied by turbulence, causing low coherencies in internal wave cross-spectra, and (4) the conclusion that the results given here represent an observation of the interaction of one part of an internal wave spectrum with another part.

## ADMINISTRATIVE INFORMATION

APPROVED AND RELEASED 3 OCTOBER 1966

H. H. Jasper, Dr. Eng.
Technical Director

J. D. W. Borop, CAPT, USN
Commanding Officer and Director

# Best
# Available
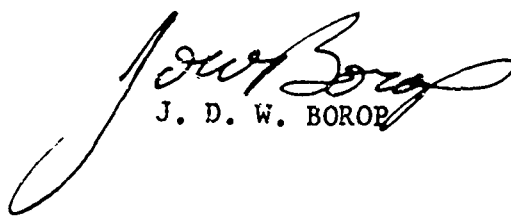# Copy

**U. S. NAVY MINE DEFENSE LABORATORY**

PANAMA CITY, FLORIDA

IN REPLY REFER TO
Code 713

From: Commanding Officer and Director
To: Distribution List

Subj: MDL Unclassified Report 313 of November 1966; information concerning

1. The purpose of this report is to document the results of experimental and theoretical investigations on the subject of shallow-water internal waves in the ocean. This work was undertaken in order to explore and understand the nature of internal wave-induced thermal fluctuations in the sea.

2. Results of this work indicate that thermal fluctuations associated with shallow-water internal waves are accompanied by fluctuations resulting from mutual interaction of the internal waves, horizontal shear flows, and turbulence. In general, it will not be possible to treat internal waves and turbulence as separate effects in studies of sound transmission through nonhomogenous oceans.

3. Results of this work indicate that linear internal wave theory adequately describes the basic internal wave motion observed experimentally. The use of spatial cross-spectral analysis technique is required to establish the presence of internal wave motion. A more comprehensive nonlinear theory is needed to account for interaction of internal waves, shear flows, and turbulence.

4. This report is made in order to document the technical information contained herein and is forwarded for information to interested activities.

J. D. W. BOROP

TABLE OF CONTENTS

LIST OF ILLUSTRATIONS

# INTRODUCTION

This report presents the findings of a three-day internal wave survey at Panama City, Florida. The purpose of this survey was to investigate the existence and characteristics of internal waves in this nearshore area during maximum summer stratification and in the presence of strong resonant internal tides.

If one considers two layers of immiscible fluids (such as oil and water), with the less dense liquid on top, it is possible to show that waves can be excited which travel along the boundary between the liquids. Such waves are called internal waves because the region of maximum vertical motions is in the interior of the fluid; little or no motion occurs at the visible upper surface. In the examples just given, the waves are also known as interface or boundary waves, because the motion is confined mainly to the sharp interface between the fluids. In the oceans it is not possible to establish and maintain such discontinuous layers, and the density generally increases downward in a smooth fashion. Internal waves which occur on such a continuous density gradient are called body waves, and form the subject of this report. Oceanic internal waves generally have wavelengths, periods, and amplitudes much larger than do ocean surface waves (note that ocean surface waves themselves are rather extreme examples of interface waves); on the other hand, internal wave speeds are much slower than surface waves. It is difficult to visualize and "get a feel for" internal waves with periods measured in hours, wavelengths in kilometers and amplitudes of the order of 10 meters; to measure and analyze such waves, in the presence of other obscuring motions, is no trivial matter.

The problem of obtaining, understanding, and applying oceanic internal wave data has perplexed oceanographers for the last half century, in fact, at a special meeting of the Conseil Permanent International Pour L'Exploration de La Mer in 1931, it was stated that the subject of internal waves" . . . had increased enormously in importance and now was the main point in modern hydrography" (Reference 1). As indicated in the excellent review of the subject by Lee (Reference 2), there has been a recent steady increase in internal wave research, particularly during the last decade. In spite of this upsurge of activity, another statement made during the meeting previously referred to (Reference 1) unfortunately remains true: " . . . the important investigations on internal waves of the last 20 or 30 years have chiefly

raised questions rather than solved them. We want very badly not only a fuller empirical knowledge of the matter but also a real understanding of the dynamical causes of the waves. In both directions there is--even on essential points--very much left to do." Contributing to this situation are three main factors, which will be discussed in relation to the present status of internal wave research, and also in relation to results presented in this report.

1.  The interior of the ocean is a good hiding place. Unlike ocean surface waves, internal waves are never directly observable by either human senses or direct techniques such as stereophotography. In the absence of such direct observations, interpretation of instrumental observations is often ambiguous. A common problem of this type has been the interpretation of irregular or quasi-periodic thermal and density fluctuations in terms of Fourier components; it is usually not possible to assign the components unambiguously either to a wave motion spectrum or a spectrum due to turbulence. In this report the attitude is adopted that if there are measurable free internal waves, data must result which satisfy the characteristic frequency-wave number equation from internal wave theory. Implied in this attitude is the necessity of using a continuous density versus depth model instead of a discontinuous layered model.

2.  The basic linear theory for internal waves in continuously stratified media has been well developed and explored only for simple cases, e.g., for exponential variation of density versus depth, for plane-parallel boundaries, and no vertical boundaries. Although more complicated three-dimensional models utilizing discontinuous layers have been explored (References 3, 4, and 5), a search of the literature indicates that theory has not been developed for the three-dimensional nearshore shallow-water problem with coastal boundaries, sloping bottom, rotation, and continuous density variation. Solutions for this difficult but more realistic boundary value problem, although badly needed, are likely to be very difficult to interpret and relate to experimental data. With few exceptions (References 6 and 7) nonlinear effects such as surface-internal wave, internal-internal wave and internal wave-bottom interactions have not been studied theoretically. It is becoming evident that such phenomena cannot be neglected for even a gross understanding of the dynamics of internal waves in shallow water.

In this report the linear theory of Tolstoy (Reference 8) is extended to a density versus depth relation which is more realistic than the usually used exponential relation; however, the effects of vertical boundaries and nonlinearities are not treated.

3.  The mutual interaction of internal waves and turbulence, especially when associated with shear flows, is probably the most

critical unsolved problem area for understanding of nearshore internal
wave dynamics. One view of this problem is to consider that shear
flows produce turbulence, and that by definition there are shear flows
involved in internal wave motion; thus one might expect that the long
wavelength, low-frequency part of the internal wave spectrum could pro-
duce shears that would affect the shorter and slower moving waves in
the high-frequency part of the spectrum. In fact, for a perfect
incompressible fluid in a two-layered discontinuous system (with no
interfacial tension), it is easy to show that, for any small but finite
shear flow, there is a frequency above which internal waves will be
destroyed. The physical effect involved is analogous to the shearing-
off of surface wave peaks by a following wind of velocity greater than
the wave velocity. One would expect that turbulence would result from
such destruction of internal waves by shear flow. Criteria and theory
for quantitative analysis and prediction of such instability and
resulting turbulence for a model with continuously varying density are
not well developed, even at the linear, small amplitude level. On the
other hand, it is well known (References 9 and 10) (at least in the two-
layer case) that for some range of shear velocities, stable internal
waves can form and propagate; at higher values of shear velocities,
the waves dissipate and mixing ensues. Thus it may be expected that in
the real ocean, if large-scale time varying shears are present (e.g.,
due to internal tides at the low-frequency end of the internal wave
spectrum), these shears may at some times generate internal waves but
at later times destroy some portion of the waves (and produce turbulence)
at the high-frequency end of the spectrum. One implication of such a
concept is that internal waves of certain frequencies would not be
stationary over periods of several days, and that coherencies observed
from averages over such periods would be drastically reduced due to the
"turbulent" parts of the alternating wave-like and noise-like sections
of resulting data records. Since averages over many waves are required
to establish statistically valid coherencies, it is apparent that either
the reduction in coherence caused by turbulence must be accounted for
(if it is shown to be significant) or other means must be devised to
analyze for internal waves. It is significant to note that essentially
all internal wave spectra reported in the literature are similar in
shape to spectra of turbulence, and coherencies observed over distances
less than one wavelength are always significantly lower than can be
accounted for unless turbulence effects are present; however, until
now no definite mechanism has been postulated to relate turbulence
effects to the internal waves. In this report observational data are
presented which are consistent with the idea that internal waves and
turbulence are inextricably interwoven through interaction of tidal-
frequency shears, vertical density gradients, and the dispersive nature
of internal waves.

In a recent interesting report, Black (Reference 11) presents
evidence, based on consideration of nonlinear effects, that

" . . . internal waves, if they exist, are in equilibrium with the turbulence and indeed are caused by the turbulence." His analysis shows that (1) particle velocities associated with long internal waves are about equal to expected velocities due to turbulence, and (2) turbulent velocities of the order of 10 percent or greater of internal wave phase velocities result in the destruction of wave motion in a time of the order of one wave period. Based on these results, he concludes that temperature fluctuations should probably not be interpreted as the superposition of internal waves, due to loss of coherency within one wavelength. Thus, on the basis of Black's analysis, neither internal waves nor turbulence should be expected to exist solely or separately in a stratified medium with shear flow, with the corollary that internal wave coherencies should be low. As will be seen, data presented here are consistent with these ideas.

## INTERNAL TIDE

Before beginning consideration of experimental and theoretical results, the internal tide which occurs in the Panama City region will be briefly discussed because of its role as a large-scale energy source at the low-frequency end of the internal wave spectrum.

Since Panama City is located near 30°N latitude (Figure 1), and has diurnal surface tides (as shown by Figure 2), the tidal period is essentially one-half pendulum day; put another way, the inertial response period is the same as the tidal forcing function period. As is well known from internal wave theory, if effects of earth rotation are included, a resonance occurs when the frequency is the same as the half-pendulum day frequency. Observations (Reference 12) of thermal structure near Panama City over a period of several years indicate that such resonant effects do occur whenever the water column has positive stability. Figure 3 (from Reference 12) shows an example of the type of thermal fluctuations which occur consistently during summer months when vertical temperature gradients range from 1/5 to 1°F per foot. Although the mean surface tide range is only 1.3 feet, the internal tide range is 20 to 30 feet. The internal tide increases and decreases in amplitude fortnightly as do the surface tides. Current measurements indicate that when the surface tide is rising, water above the thermocline has an offshore component, while water below the thermocline is flowing onshore at a rate sufficient to increase the total water depth. In this process the thermocline region is raised more than ten times as far as the surface, thus causing the observed vertical fluctuations of the thermocline.
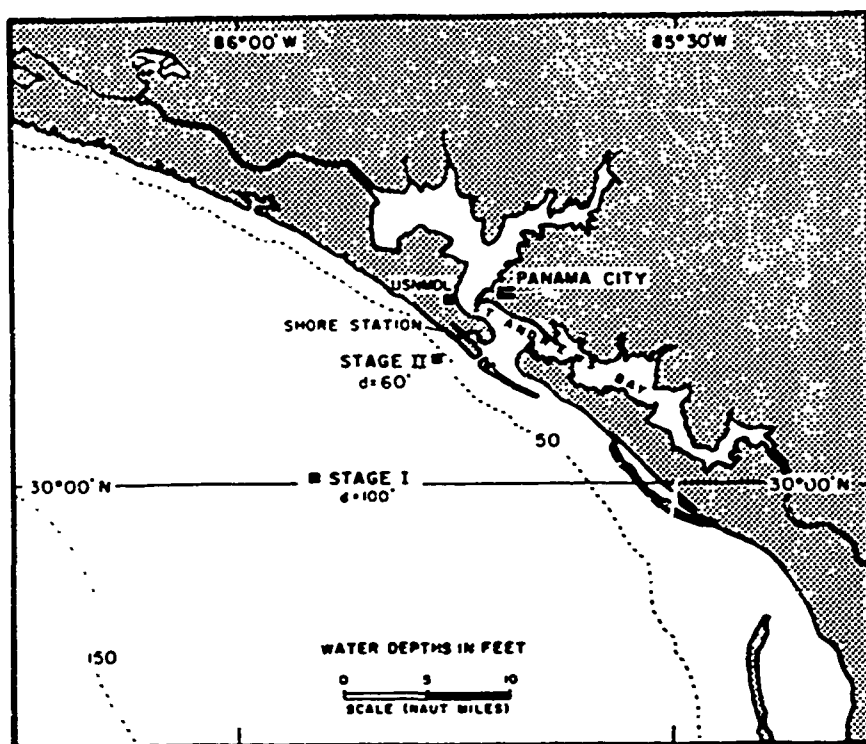
FIGURE 1. LOCATION CHART OF STUDY AREA OFF
PANAMA CITY, FLORIDA

Y-axis (top graph): HEIGHT IN FEET — 3, 2, 1, 0
X-axis: 12, 24, 12, 24, 12, 24, 12

THE SURFACE TIDE AT STAGE I

| JUNE 19 |      JUNE 20      |      JUNE 21      | JUNE 22 |

Y-axis (bottom graph): HEIGHT IN FEET — 3, 2, 1, 0
X-axis: 12, 24, 12, 24, 12, 24, 12

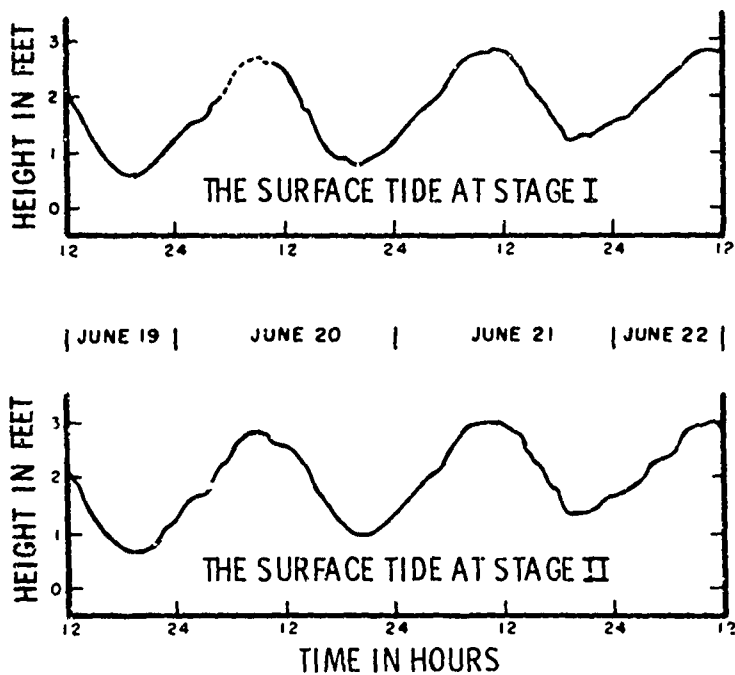THE SURFACE TIDE AT STAGE II

TIME IN HOURS

FIGURE 2.  TIDE RECORDS AT STAGE I AND STAGE II
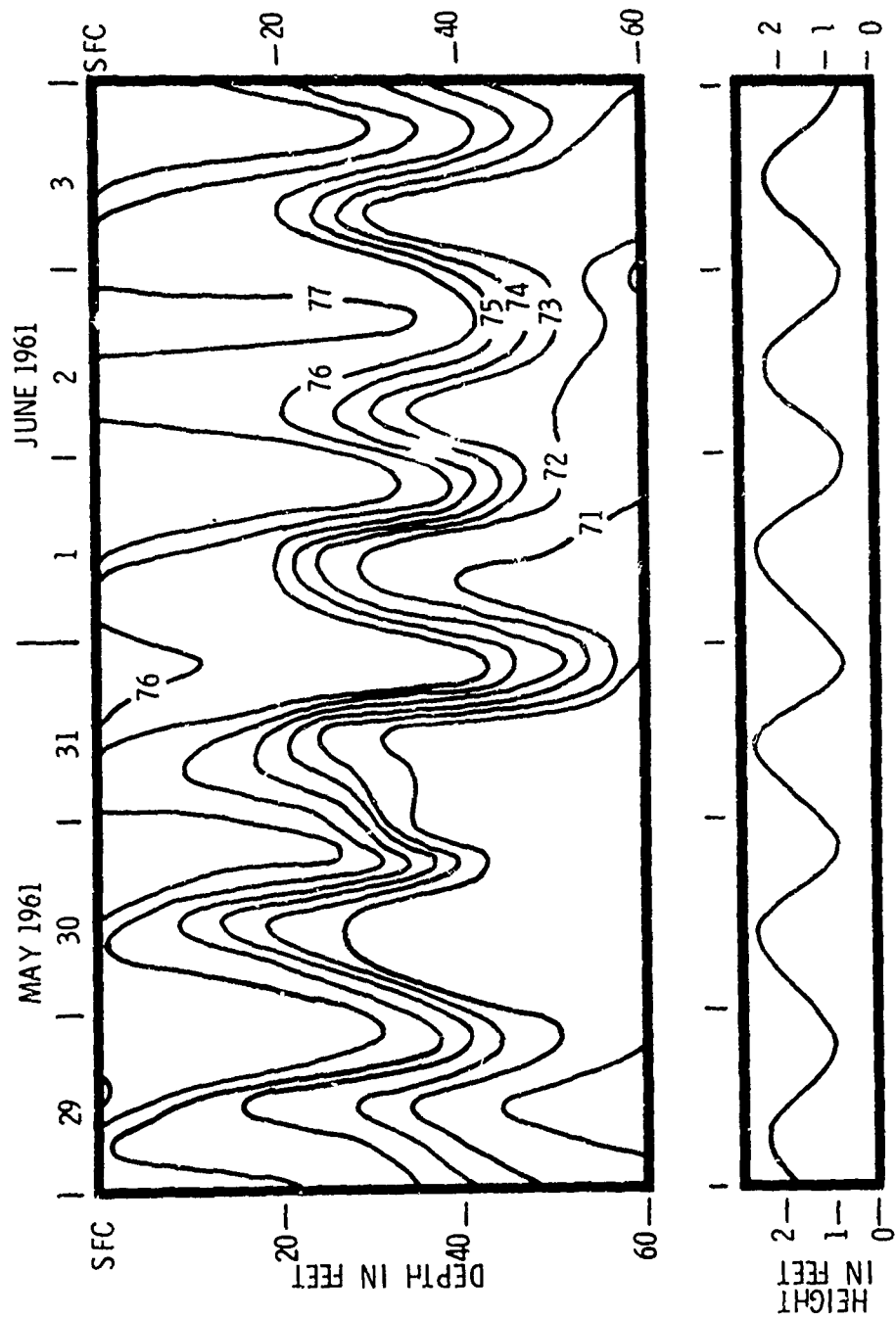FROM 1200 JUNE 19 TO 1200 JUNE 22, 1962

8

FIGURE 3. PREDICTED TIDES

The linear theory of internal tides, for a rotating, two-layer, coastally-bounded ocean with a continental shelf (References 3, 4, and 13) predicts two basic types of possible wave motion for internal tides: standing waves and edge waves. In the standing wave solution the internal tide is generated at the edge of the continental shelf and reflected from the coastal boundary, causing standing waves in the region between the coast and the shelf edge. In the edge wave solution, there are "trapped" waves traveling along (i.e., parallel to) the coastal boundary, with amplitudes decreasing exponentially from shore. Due to the long wavelengths involved at tidal frequencies (i.e., of the order of 50 km or more), use of a discontinuously layered model is justifiable. Long wavelengths also mean that data adequate to resolve the structure and dynamics of resonant internal tides must span distances comparable to the wavelengths. Such data are not presently available from the northeastern gulf region. Boston (References 14 and 15) has investigated the internal tides in the Panama City area using data from the survey reported herein. His conclusions (Reference 15) are as follows:

"The vertical oscillations of the thermocline observed off Panama City are due to horizontal tidally induced movement being translated to vertical motion, through coupling with the bottom topography. The tidal coupling weakens in the offshore direction as the depth increases. The coupling weakens shoreward first in the upper layers and then in the lower layers. The mechanism proposed is that of an internal edge wave of the same period as the surface tide towards the northwest. The length of this wave is probably much less than the wavelength of the tidal wave. The effect of this wave far from shore is neglibible and it is suggested that observations at nearshore stations may shed little or no light on the coastal generation of internal waves of tidal period over the continental shelf. Comparison of these observations with observations made off a coast with widely differing shelf characteristics indicated some similarities, but information was insufficient for detailed comparisons. It is significant that in both cases the thermoclines were observed to intersect the bottom. This feature has been ignored in all theories regarding the effect of coastal boundaries on internal waves. The reason for the omission is simple; namely, its inclusion complicates the mathematics of an already complex mathematical problem. In particular, the effect of this modification on the second model proposed by Rattray (1960) and the model of Iida and Ichiye (1963) should be investigated. It is believed that further study of two-layer models incorporating intersection of the thermocline with the bottom and boundary conditions such as shown in Figure 18 will aid in understanding the gross features observed off Panama City, Florida. If a more specific understanding of the motion of the thermocline is desired, then the two-layer model must be replaced by at least a three-layer system such as two isothermal layers separated by a linear thermocline."

10

Boston's proposal that the internal tide is an edge wave implies that
the surface tide is also an edge wave. The nature of the surface tide
in this region is, unfortunately, not well enough understood to deter-
mine its type. Resolution of detailed structure and dynamics of the
locally resonant internal tide awaits data collected over larger spans
of distance and time than has been done previously.

Two significant features of the observed internal tide are worth
noting. First, the internal tides apparently do not "break" at their
shorelines. The thermocline is observed to be continuously stable into
the region at which it intersects the bottom. Direct observations (via
scientific diving techniques) of the "thermal shoreline" have been made;
it is possible to find the region at which a diver, with arms hori-
zontally outstretched along the bottom, can have one hand (offshore)
in a layer of water several inches deep which is several degrees colder
than water at his other hand (nearshore). In this manner the thermocline-
bottom intersection can be localized to within several feet. Such obser-
vations have been made only during summer months, when the thermocline is
well developed (approximately 10°F difference across thermocline); during
spring or late fall when the thermocline is weak, there may be thermal
"breaking" near shore. The observation that internal tides do not break
implies that shoreward wave number components will be essentially per-
fectly reflected, leading to standing waves.

The second significant feature of the internal tides concerns the
shear currents associated with internal tidal motion. Measurements
indicate that the upper and lower well mixed layers of water move with
different speeds and directions, causing low frequency (1 cycle per 24
hours) large scale (of the order of 50 km) shear motions. These shear
motions are superimposed on motions due to higher frequency internal
waves, and can affect their behavior and stability. Figure 4 shows the
measured net shear vector variation as a function of time during the
survey. The net shear vector rotates clockwise with the tides, has
generally somewhat larger magnitudes in the alongshore direction than
offshore, and exhibits large and irregular variations in magnitude.
Measured current speeds in the surface layer were always larger than in
the bottom layer; it can be seen that the surface current generally has
an offshore component during the time between low- and high-surface tides
(as indicated by L and H on Figure 4). No further attempt is made in
this report to resolve details of the internal tide structure; however,
effects of internal tides and associated shears will be pointed out in
subsequent sections.

FIGURE 4. VARIATION OF CURRENT SHEAR VECTOR
VERSUS TIME, STATION M3

## DATA COLLECTION AND ANALYSIS

Observational data were collected from locations shown in Figure 5. On the right is shown the shoreline of the Panama City Beach area, and the entrance channel leading to St. Andrew Bay. About 1.5 miles from shore is the Mine Defense Laboratory offshore platform, Stage II (S2), forming the shoreward end of a line of fixed data collection stations. At the seaward end is Stage I (S1). Between S1 and S2 were stations M1, M2, M3, and M4, occupied by vessels fixed in two-point moors. Also shown are station locations A0 through A9 and F0 through F9, which were visited serially by mobile vessels. This report is based mainly on data gathered from Stations S1, M1, M2, M3, M4, and S2. Notice that the fixed station line spans water depths of 60 to 100 feet in topography that is generally smooth.

At all stations along the fixed station line, except for S1, bathythermograph (BT) casts were made synchronously every 15 minutes for a period of about 72 hours between 1200, 19 June 1962 and 1500, 21 June 1962. Bathythermographs used were specially modified to provide full-scale depths of 60 and 100 feet. Water samples for salinity were taken at all stations on an hourly schedule. Current measurements on 1-hour and 2-hour schedules were made at all fixed stations with Ekman meters and current drogues. At A1, the Texas A & M automatic data collection system (Reference 16) recorded temperatures at six depths, currents at three depths, and meteorological data: these data were recorded once per second over about half of the survey period. Water level recorders and tide wells were installed at S1 and S2 to record surface tides, producing results shown in Figure 2.

Meteorological and sea state conditions were generally calm during the survey period. Significant wave heights never exceeded 3 feet (90 cm), and averaged less than 1 foot (30 cm). Wind speed averaged less than 10 knots (5 m/sec), with highest speeds occurring in one 4-hour period of squalls during one night. Thus, except for solar radiation, energy inputs from boundaries were small during the survey period.

The approximately 1500 BT slides from the survey were processed, error-checked and corrected. Reduced data from each slide were recorded as temperature at 5-foot (1.5 m) depth intervals and the depth at which integral values of temperature occurred. After final correction, all BT data were entered on punched cards for computer processing. Salinity samples and current data were processed and tabulated for further analysis.

This report is based mainly on analysis of isotherm depth versus time data. Ten isotherms (74° to 83°F) resulted at all stations except
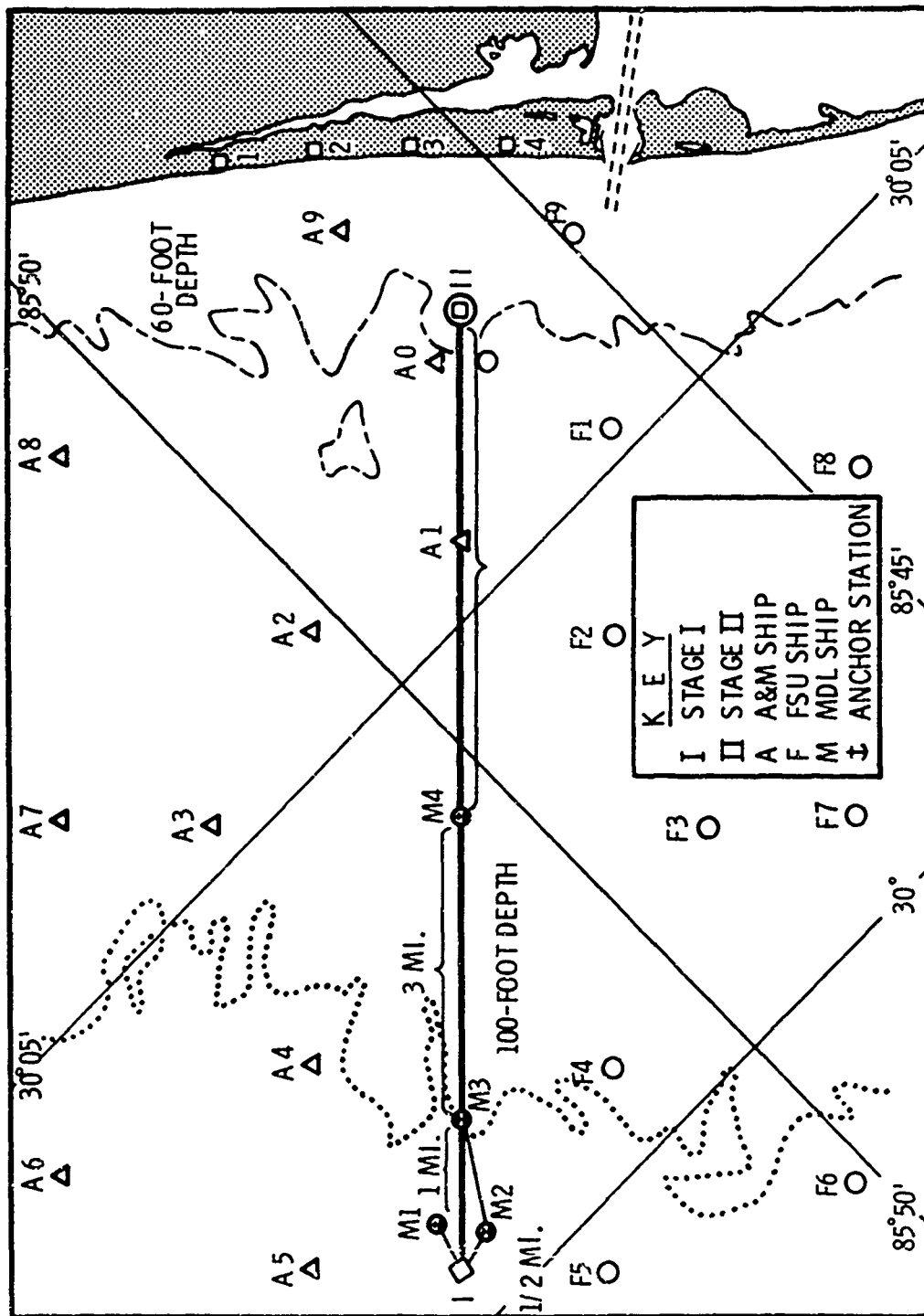
FIGURE 5. STATION PLAN

14

for S2, which had five (79° to 83°F). The raw isotherm data are shown in Figures 6, 7, 8, and 9. These are presented to show both the general nature of the isotherm fluctuations and also the internal tide. (With the exception of S2, every other isotherm has been omitted for clarity.) The internal tide appears most strongly at the nearshore location of S2 and diminishes seaward. Note that the internal tide does not appear to be a simple first mode disturbance, especially at S2; the thermocline alternately expands and contracts vertically, resulting in a substantial time variation of water column stability. These effects become less pronounced seaward but are still observable. Superimposed on the internal tide fluctuations are irregular higher frequency variations which are not obviously wave-like in appearance, but for which an internal wave analysis was made. It was apparent from the outset that the internal wave field was of the same nature as surface waves, i.e., random and confused. It also seemed probable that internal waves and turbulence coexisted so that effects of turbulence could not be ignored. Because of these effects, it was not possible to trace individual disturbances from station to station, and a statistical analysis was necessary.

Each isotherm was fitted by least squares to a straight line, yielding average isotherm depth and its trend with time. Changes in average isotherm depth with time were negligible for the data subjected to analysis. Because of this and the fact that the variance of each isotherm was reasonably constant over its time span, the data were considered sufficiently stationary for time series analysis.

Cross power spectral analysis was done for:

1. All possible pairs consisting of each isotherm at one station crossed with the same isotherm at all other stations, and

2. All possible pairs consisting of one isotherm within a given station crossed with another isotherm of the same station. Plots were made of isotherm power spectra, phase, and coherence versus frequency. The power spectra were plotted as log power versus linear frequency and also versus log frequency. The spectral analysis program used is described in Reference 17, and has the following pertinent features: (a) prewhitening is used, (b) a least square linear trend is removed from the input data, and (c) the lag window used is that due to Parzen (Reference 18).

Confidence limits associated with estimates of spectral density, phase, and coherence depend upon the number of equivalent degrees of freedom, $\nu$, which, according to Reference 18 is 3.7 times the sample size divided by the number of lags for the lag window used. For the data presented here, the sample size is 296 and the number of lags is 24,
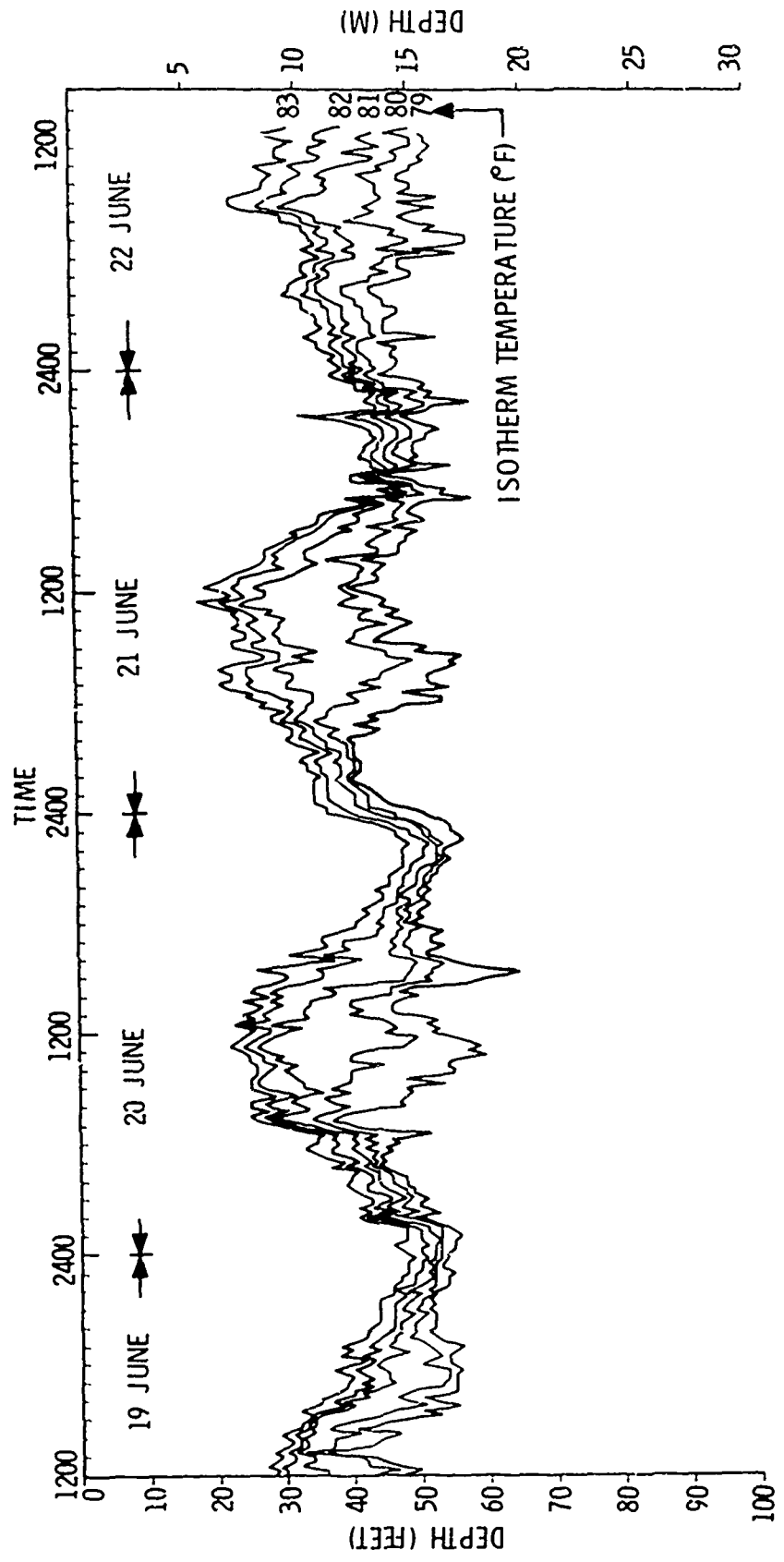
15

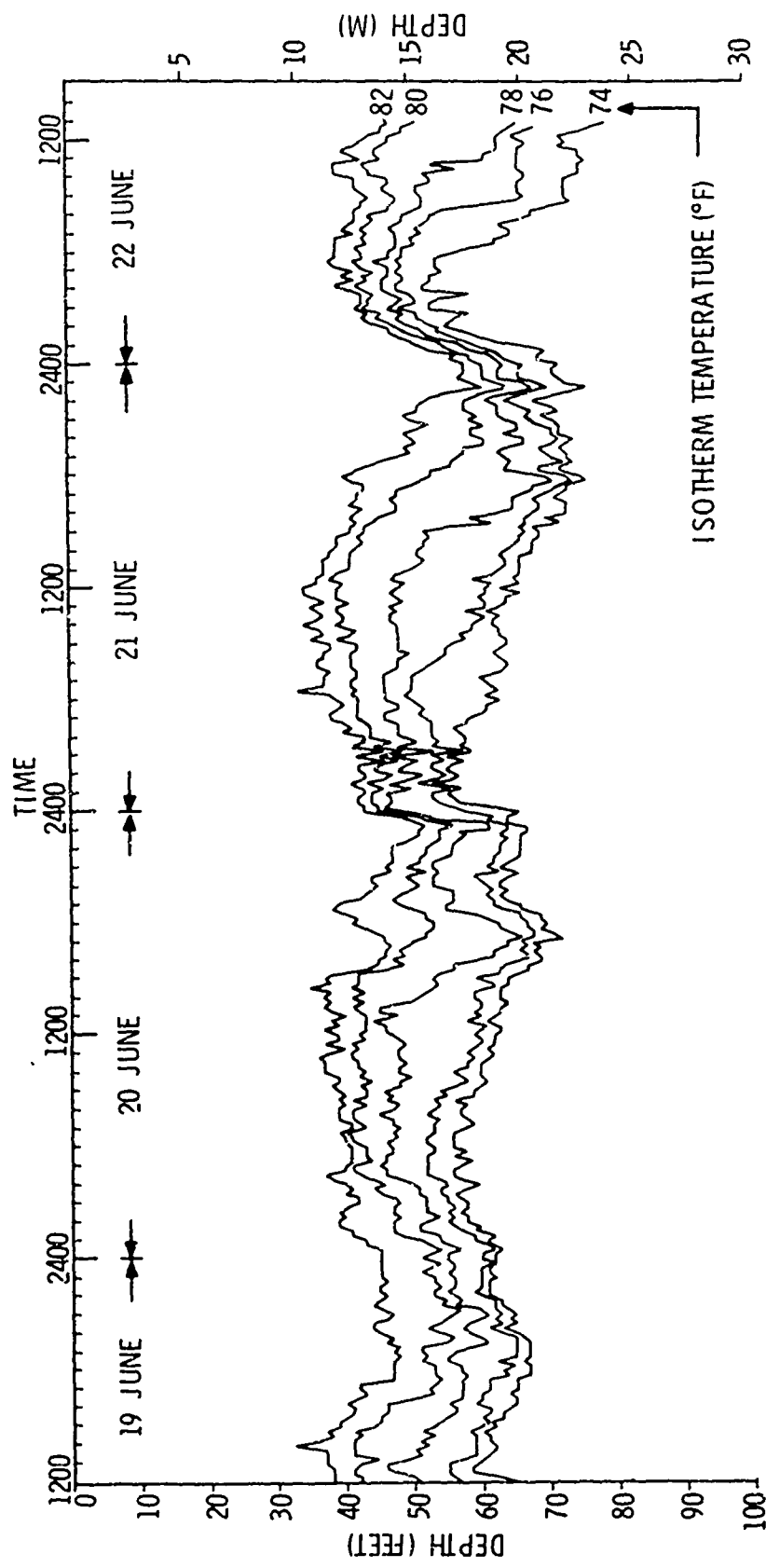FIGURE 6. ISOTHERM VARIATION VERSUS TIME, STAGE II

16

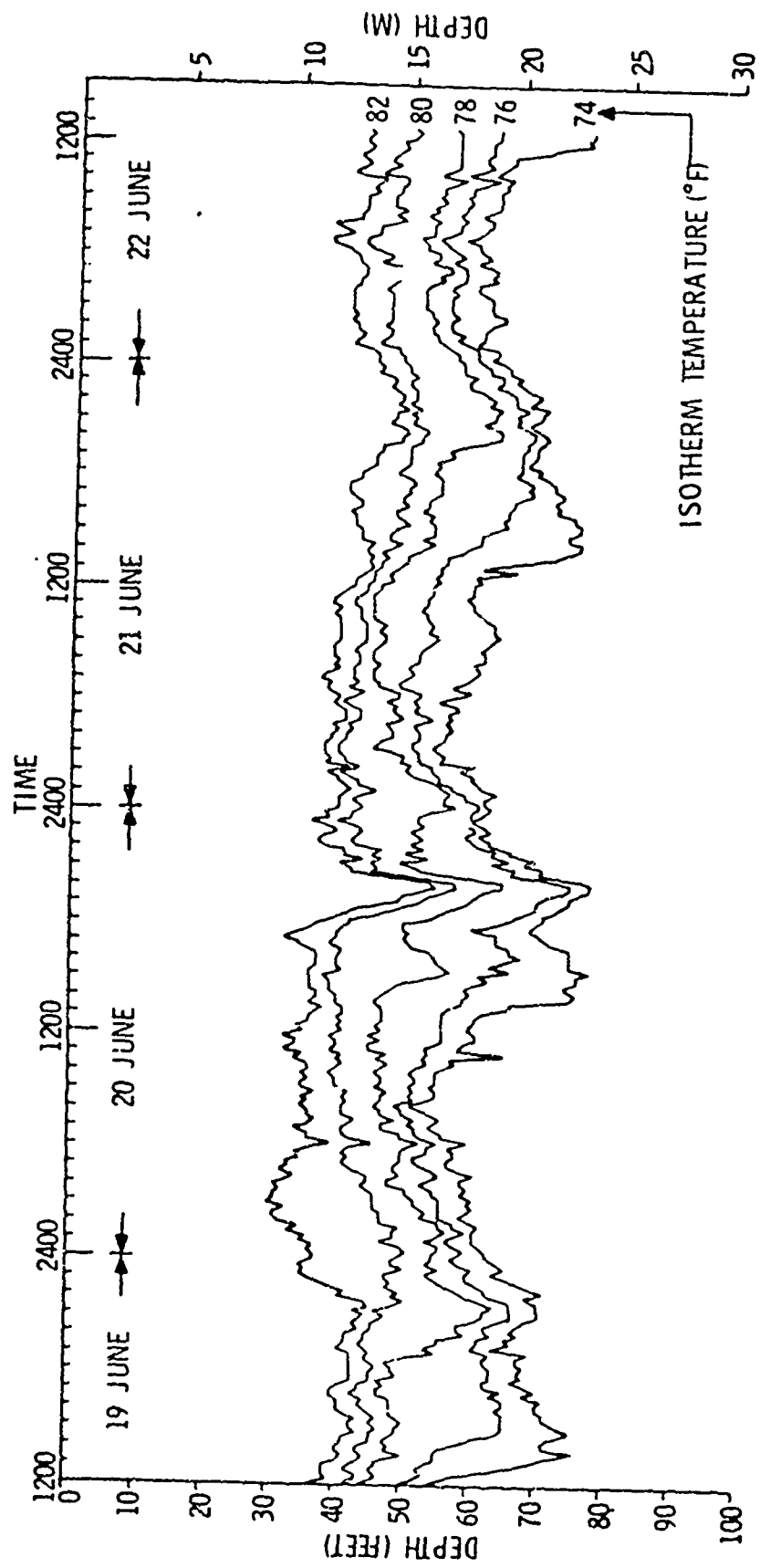FIGURE 7. ISOTHERM VARIATION VERSUS TIME, M4

17
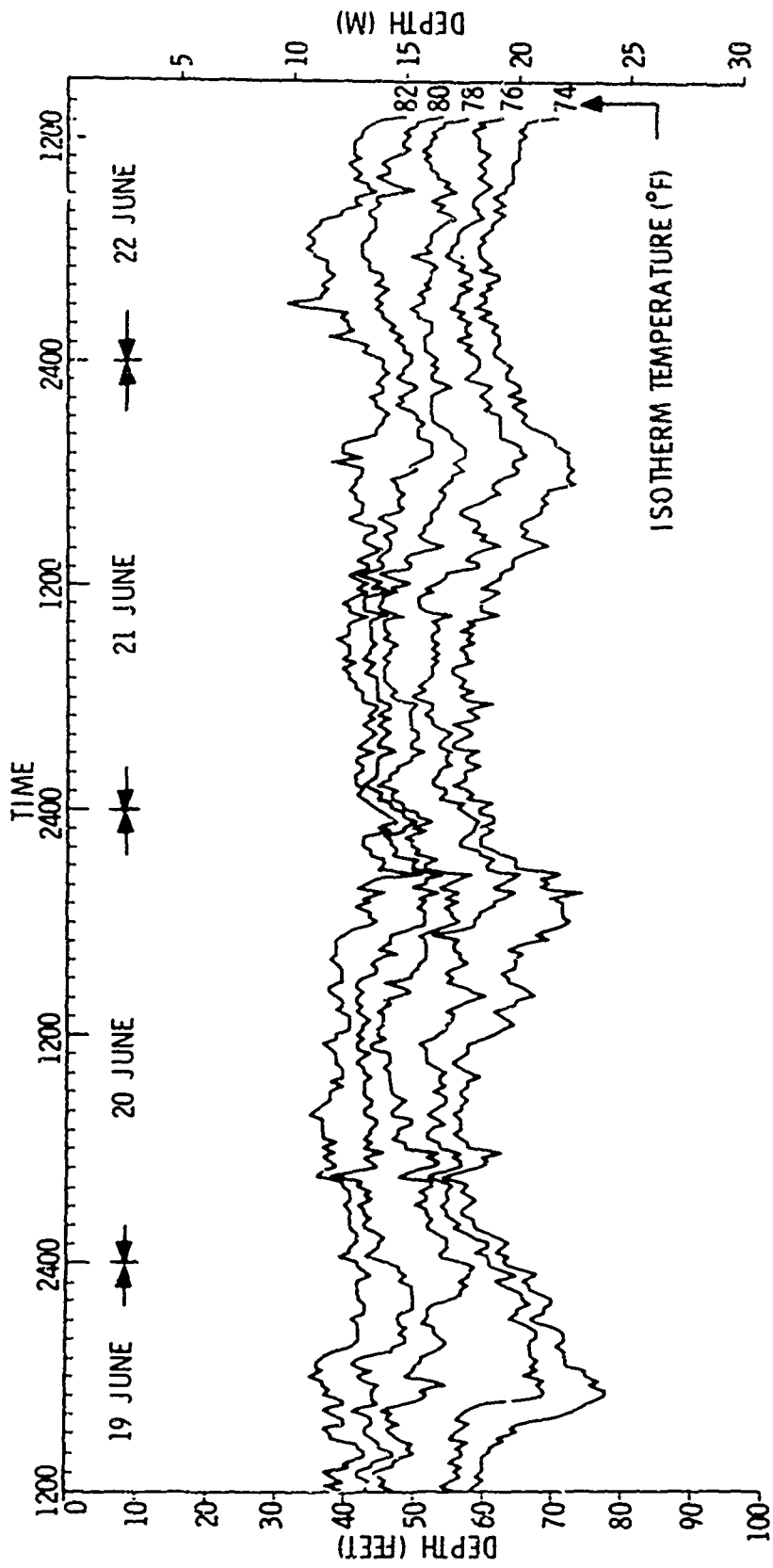
FIGURE 8. ISOTHERM VARIATION VERSUS TIME, 1983

18

FIGURE 9. ISOTHERM VARIATION VERSUS TIME, M2

yielding 45 degrees of freedom. Confidence limits for estimates of spectral density and phase were determined using data from Reference 19 and for coherence from Reference 20.

The maximum frequency for which power spectra yield information is the Nyquist frequency, $F_n$, determined by $F_n = \frac{1}{2\Delta T}$, where $\Delta T$ is the sampling interval. In this case, $F_n = \frac{1}{30} = 0.033$ cycles per minute. Because internal waves can exist at higher frequencies, aliasing of higher frequency energy down into the (lower frequency) analysis band could possibly cause errors. As will be shown later, for the present results, the high-frequency energy is sufficiently small compared to the experimental noise level in the analysis band that aliasing is not a problem. The lower limits on spectral energy estimates are determined by the overall BT reading error for isotherm depth; this error was, on the average, about 5 to 6 feet (1.5 to 1.8 m) (rms) corresponding to a spectral level of about 25 to 36 feet squared (2.2 to 3.2 meters squared).

## DENSITY PROFILES

The average isotherm depths were combined with salinity data to compute average density profiles at each station. The results indicated that the average density profiles were essentially the same at all stations over the three-day period, with the lower portion of the profile being cut off by the bottom in shallower depths. The average density profile is shown in Figure 10, where both depth from the surface and the vertical coordinate, z (positive upward with origin at depth of 100 feet), are shown. The coordinate, z, will be used in theoretical considerations to follow.

Basic to the existence of internal waves is density stratification, i.e., density is a nonconstant function of the vertical coordinate, written as $\rho(z)$. Since the vertical density distribution function $\rho(z)$ of the undisturbed water column is so important in applications of internal wave theory, an effort was made to fit the measured distribution shown in Figure 10 by an analytic function. As can be seen in the figure, the data are well represented by

$$\rho(z) = 2 \times 10^{-3} \left[ 1 - \tanh \frac{2}{32} (z - 47) \right] + 1.02045 \tag{1}$$

where $\rho(z)$ is in gm cm$^{-3}$, z is the vertical coordinate, the number 47 represents the vertical coordinate of the mid-density point, and the number 32 in the denominator of the hyperbolic tangent argument is a
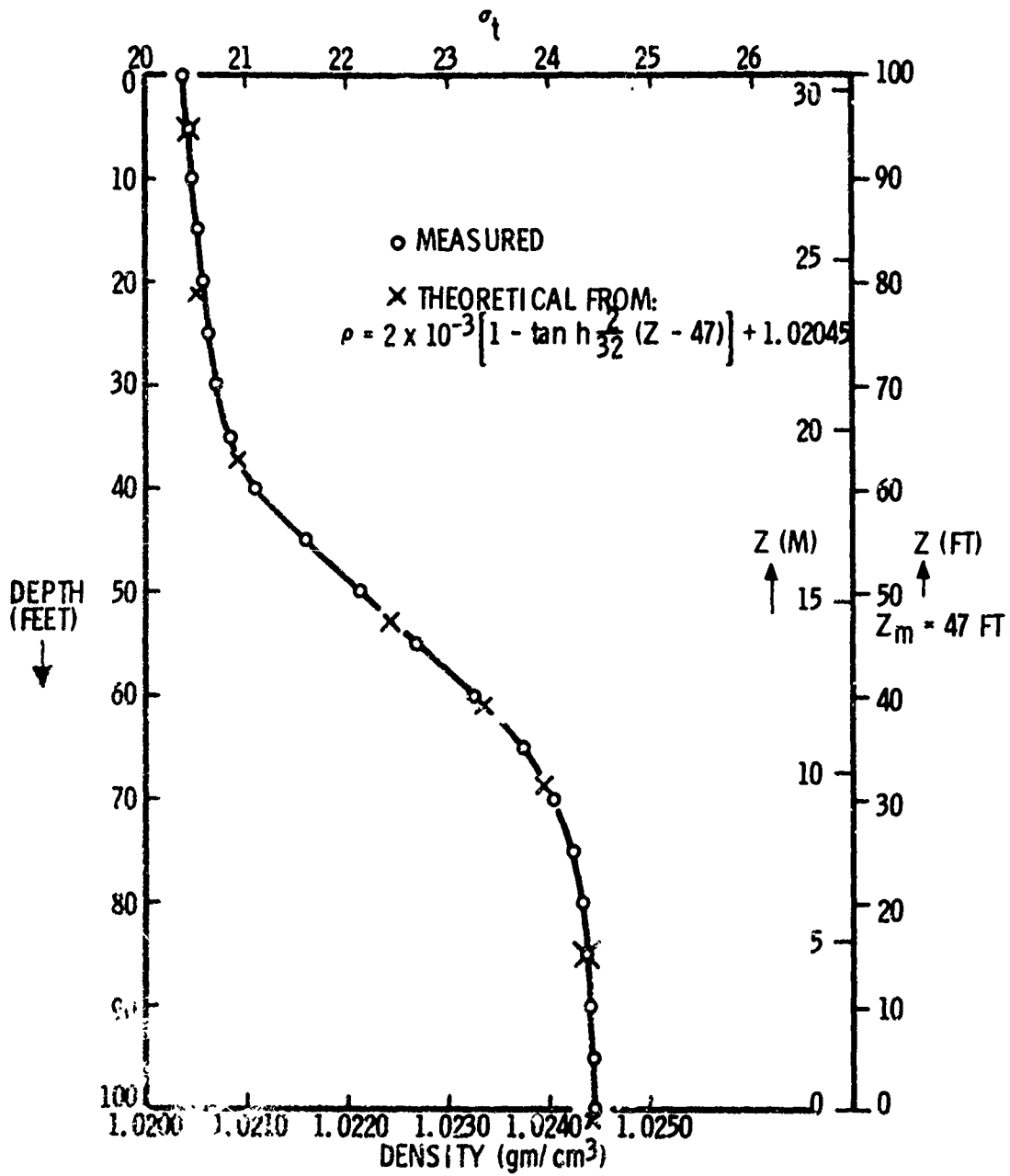
20

FIGURE 10. DENSITY VERSUS DEPTH
AVERAGE, M2, M3, M4, SII

21

convenient measure of the thickness (in feet) of the transition layer between the well mixed upper and lower layers. The density profile observed in this work agrees well with results of Lofquist (Reference 9) in a laboratory study of flow in stratified fluids. In Reference 9, a two-layer (fresh and salt water) system was sheared to determine the characteristics of the interface between layers and the vertical density distribution as a function of shear velocity profile and magnitude. Sixty-nine experiments spanning a wide range of density differences (stability) and interface characteristics (ranging from plane through wavy, to very agitated) all produced density distributions well described by a function of the form of Equation (1). Lofquist concluded that since the density profiles were found to be quite regular and permanent, in spite of mixing, the density profile depends mainly on the fluid properties and flow characteristics, but not on the history of the flow; however, he pointed out that he did not know if this conclusion would be valid for oceanic scale phenomena because of the relatively small values of Reynolds number ($<2 \times 10^4$) in his experiments. Results of the present survey tend to confirm his conclusion and also suggest that there may be some universal profile to which the density distribution adjusts under two-layer shear flow conditions in absence of significant energy input through the boundaries. This conjecture appears to warrant theoretical or experimental confirmation.

Implied by the steady state density profile of Equation (1) is a mechanism necessary to remove mixed liquid away from the transition region, for if such removal did not occur, the density profile would steadily change. Such a mechanism may be provided by the turbulence associated with the shear flow induced by internal tides. Also necessary, of course, is a steady energy input to restore the stability destroyed by turbulent mixing and vertical convection. Solar radiation is a mechanism sufficient to cause both a steady but slow increase in total surface-to-bottom density difference and also a steady increase in water column temperatures throughout the summer months (Reference 22).

Since internal waves transport energy but not matter, it is difficult to visualize how internal wave motion alone could either produce or maintain the observed average density profile.

Thus, by observing the equilibrium density distribution, one is led to the expectation that both internal waves and turbulence should be present and probably interacting in a complicated manner, on the following basis: (1) necessary conditions for existence of internal waves are the presence of a density gradient and an energy source such as flow or pressure perturbations associated with turbulent oceanic motion on a large scale; (2) such an energy source is provided by resonant internal tide shear flow; and (3) turbulence associated with internal wave shear flow interacts with and maintains the equilibrium density gradient upon which the existence of internal waves depends.

On this basis, the internal wave field becomes part of the mechanism for dissipating large-scale energy inputs arising from tides and insolation. The details of the chain of physical effects outlined above remain to be worked out; no satisfactory theory exists to describe the interaction of internal waves and turbulence, nor does there exist an adequate theory for agitated interfacial flow in a two-layer system.

We now turn to the question--in view of the fact that we expect internal wave data to be contaminated by turbulence effects, what evidence is required to establish the coexistence of internal waves and turbulence?

## THEORETICAL AND EXPERIMENTAL RESULTS

Tolstoy's (Reference 8) comprehensive theory of waves in strati-fied fluids forms the basis of our theoretical study of internal waves; we extend Tolstoy's theory to include the case of a density gradient described by Equation (1). The theory is linear and includes the effects of continuous stratification, gravity, rotation, and presence of horizontal upper and lower boundaries. It does not include the effects of viscosity, heat conduction, vertical boundaries, or compressibility.

The approach used by Tolstoy to develop equations describing inter-nal waves is somewhat different from the usual approach which starts with the linearized equations of fluid mechanics, and ends with second order differential equations for fluid velocity components. Tolstoy uses a variational approach which results in equations for the dis-placements from equilibrium, which are directly measurable and intuitively visualizable quantities. Tolstoy shows that these equa-:ions are completely equivalent to those resulting from the first order perturbation form of Euler's equations of fluid dynamics; they are also identical to equations obtainable from Biot's theory for waves in prestressed elastic media (Reference 22).

Although a complete derivation of the equations will not be given here (since this is done in Reference 8), a brief recapitulation is p.esented of Tolstoy's approach, along with the resulting equations which form a starting point for the theory used in this report.

A stationary Cartesian coordinate system x, y, z, is used, with the vertical axis z positive upward and the gravity field vector $\vec{g}$ downward. Let $\xi$, $\eta$, $\zeta$ be the x, y, z components of displacement of a fluid element from equilibrium, and $\rho(z)$, the equilibrium density of the fluid, be a function of depth only.

23

A Lagrange density function is derived which is the sum of terms involving kinetic energy, potential energy, elastic energy, gravitational energy, and effects of compressibility. Application of this Lagrange density to the Euler-Lagrange equation yields the following general equations of motion of a stratified compressible fluid in a constant gravity field, in an inertial Cartesian reference frame x, y, z, and expressing the fact that inertial forces are balanced by forces of elasticity and buoyancy:

$$\rho \ddot{\xi} - \frac{\partial}{\partial x} \Lambda \epsilon + \rho g \frac{\partial \zeta}{\partial x} = 0$$

$$\rho \ddot{\eta} - \frac{\partial}{\partial y} \Lambda \epsilon + \rho g \frac{\partial \zeta}{\partial y} = 0 \tag{2}$$

$$\rho \ddot{\zeta} - \frac{\partial}{\partial z} \Lambda \epsilon - \rho g \left( \frac{\partial \xi}{\partial x} + \frac{\partial \eta}{\partial y} \right) = 0$$

where dots indicate time derivatives, $\Lambda$ is the bulk modulus,

$$\Lambda = \rho c^2 \quad \text{(where c is the velocity of sound)}$$

and $\epsilon$ is the incremental volume change

$$\epsilon = \frac{\partial \xi}{\partial x} + \frac{\partial \eta}{\partial y} + \frac{\partial \zeta}{\partial z} \ .$$

For a rotating coordinate system there must be added to the right-hand side of Equation (2) terms involving Coriolis force components $F_x$, $F_y$, and $F_z$ (centrifugal forces are considered as incorporated in the gravity field for the localized areas considered here):

$$\vec{F} = \rho \vec{V} \times 2\vec{\omega}_p \equiv \rho \vec{V} \times \vec{\Omega} = F_x \hat{i} + F_y \hat{j} + F_z \hat{k} \tag{3}$$

where $\vec{V}$ is the fluid element velocity vector, $\vec{\omega}_p$ the planetary angular velocity, and $\vec{\Omega}$ the Coriolis vector. For the coordinate system used here Equation (3) can be given as:

$$\vec{F} = \rho \begin{vmatrix} \hat{i} & \hat{j} & \hat{k} \\ \dot{\xi} & \dot{\eta} & \dot{\zeta} \\ \Omega_x & \Omega_y & \Omega_z \end{vmatrix} \tag{4}$$

where $\hat{i}$, $\hat{j}$, $\hat{k}$ are unit vectors and $\Omega_x$, $\Omega_y$, $\Omega_z$ are components of $\vec{\Omega}$.

24

Equations (2) and (3) emphasize the dependence of fluid motions on the two basic depth dependent parameters $\rho$ and $\Lambda$, and also on earth rotation. In what follows the dependence on $\Lambda$, which ultimately is reflected in terms involving $\omega^2/c^2$ (where $\omega$ is the frequency), is negligible; thus the density function $\rho(z)$ is of major importance as the parameter which determines properties of wave solutions of Equations (2) and (3).

For $\rho$ and $\Lambda$ which are functions of $z$ only, the equations of motion (Equations (2) and (3)) are separable by assuming $\xi$, $\eta$, and $\zeta$ proportional to

$$e^{i(\alpha x + \beta y - \omega t)}$$

where $\alpha$ and $\beta$ are the x and y components of the vector wave number $\vec{K}$ (where $K = 2\pi/\lambda$, and $\lambda$ is the wavelength), and $\omega$ is the angular frequency (= $2\pi f$ where f is the frequency). With this assumption $\xi$ and $\eta$ can be eliminated from Equations (2) and (4), yielding the following second order differential equation for $\zeta$ which forms the starting point for developing the specific solutions presented in this report:

$$\frac{\partial^2 \zeta}{\partial z^2} + f(z) \frac{\partial \zeta}{\partial z} + r(z)\zeta = 0 \tag{5}$$

where

$$f(z) = \frac{d}{dz} \ln \rho(z) = \frac{1}{\rho(z)} \frac{d\rho(z)}{dz} , \tag{6}$$

and

$$r(z) = \frac{\omega^2}{c^2(z)} - \frac{k^2 [N^2(z) - \omega^2]}{\omega^2 - \Omega_v^2} \tag{7}$$

where

$$k^2 = \alpha^2 + \beta^2 .$$

The quantity N in Equation (7) is the fundamental function which characterizes the stratified medium in terms of a natural (or resonant) frequency of vertical oscillation of a fluid element, and is known as the stability (or Väisälä) frequency:

$$N^2(z) = - \left[ \frac{g}{\rho(z)} \frac{d\rho(z)}{dz} + \frac{g^2}{c^2} \right] \tag{8}$$

25

It will be seen that $N(z)$ is the maximum frequency for which free internal waves can exist at any depth $z$. Also used in Equation (7) is the quantity $\Omega_v$, which is the locally vertical component of the Coriolis vector $\Omega$; in the approximation used here, the rotation vector is considered to have only a vertical component, which is constant over the region under consideration. With this assumption we have

$$\Omega_v = 2 \, \omega_\rho \, \sin \theta$$

where $\theta$ is the latitude. For the Panama City location, $\theta = 30°$, so

$$\Omega_v = (2) \left( \frac{1}{24} \, c/hr \right) \, (0.5) = \frac{1}{24} \, c/hr \; .$$

Note that this frequency coincides closely with the diurnal tidal frequency of $1/24.8$ c/hr.

Solutions to Equations (5), (6), and (7) can be obtained through the transformation (Reference 23)

$$\zeta(z) = h(z) \, e^{-1/2 \int_z \, f(z) \, dz}$$

resulting in

$$\frac{\partial^2 h(z)}{\partial z^2} + \gamma^2(z) \, h(z) = 0 \tag{9}$$

with

$$\gamma^2(z) = r(z) - \frac{1}{4} \, f^2(z) - \frac{1}{2} \frac{\partial f(z)}{\partial z} \; . \tag{10}$$

Equation (9) has oscillatory type solutions interpretable as waves if $\gamma^2(z) > 0$. Substituting Equations (6) and (7) in Equation (10), there results

$$\gamma^2(z) = \frac{\omega^2}{c^2} + \frac{k^2 [N^2(z) - \omega^2]}{\omega^2 - \Omega_v^2} - \left[ \frac{1}{4} \frac{d}{dz} \ln \rho(z) \right]^2 - \frac{1}{2} \frac{d^2}{dz^2} \ln \rho(z) \tag{11}$$

The problem has now been reduced to finding solutions of Equation (9), with $\gamma^2(z)$ given by Equation (11) and specific functions for $\rho(z)$. At this point we note that for maximum frequencies of concern here, i.e., $\omega < 2\pi$ cycles per minute, the term $\omega^2/c^2$ (of the order of $5 \times 10^{-13}$ rad$^2$/cm$^2$) is negligible relative to the second term of Equation (11); we thus neglect the term $\omega^2/c^2$, which amounts to assuming that the fluid is incompressible, i.e., $c = \infty$. We note also that for the $\rho(z)$ functions

to be considered here, calculations show that the last two terms of Equation (11) can also be neglected without significant error.

We wish to solve Equation (9) as a boundary value problem to obtain the characteristic equation relating frequency to wave number (or wavelength); to do this, boundary conditions must also be specified. The first and most obvious boundary condition is that vertical motion at the bottom vanishes, i.e.,

$$h(z) = 0 \text{ at } z = 0 \tag{12}$$

The second boundary condition is that the upper fluid surface is either rigid or free. The problem has been solved for both conditions, with the result that there is little difference between the two situations; in what follows, the free surface condition will be used.

Solutions to the boundary value problem (Equation (9)) have been obtained for two cases of interest: the first is

$$\rho(z) = \rho_0 \, e^{-2\nu z} \tag{13}$$

where $\rho_0$ is the density at $z = 0$ and $\nu$ is a constant; the second case, matching closely the density distribution observed from data, is of the form of Equation (1),

$$\rho(z) = \frac{\Delta\rho}{2} \left[ 1 - \tanh \frac{2}{\ell_\rho} (z - z_\bullet) \right] + \rho_\bullet \tag{14}$$

where $\Delta\rho$ is the total surface-to-bottom density increase, $\rho_\bullet$ is the density at the surface, $z_\bullet$ is the z coordinate of the point at which $\rho(z_\bullet) = \rho_\bullet + \frac{\Delta\rho}{2}$, and $\overline{\ell}_\rho$ is the average value of the transition layer thickness, defined in terms of the maximum density gradient, $(\partial\rho/\partial z)$ max, as

$$\overline{\ell}_\rho \equiv \frac{\Delta\rho}{-(\partial\rho/\partial z) \text{ max}} . \tag{15}$$

Solutions using the exponential density distribution, Equation (13), have been given in the literature (References 8, 24, 25) because of the mathematical tractability resulting from this function. Only a few other specific density distributions have been considered in the literature (Reference 25); in particular, there has not been found in the literature a solution using the distribution given by Equation (14). In what follows the characteristic equation for the exponential density distribution will be discussed and used in extending the theory to the

hyperbolic tangent distribution, Equation (14). Interest will be centered on the characteristic equation, which predicts a unique relation between the measurable quantities wave frequency and wave number (or wavelength). The attitude is adopted that if there were free internal waves existing during the field survey, data should result which verifies the characteristic equation. We shall see that such is the case (although the evidence is not as strong as one would like).

For the case of an exponential density distribution, $N^2$ is a constant and $\gamma^2(z)$ is a constant coefficient in Equation (9). Although the ocean almost never has an exponential density distribution from surface to bottom, such distributions do occur over limited depth ranges. The results of using this mathematically simple model would thus be expected to have limited application. Figure 11 shows the observed average $N(z)$ variation obtained from graphic differentiation of the curve in Figure 10 and use of Equation (8). Note that the $N(z)$ curve is not constant except over portions of the thermocline corresponding to the 76° through 81°F isotherms, and over the depth range of 10 to 25 feet (3 to 7 m); over these portions, the theory for an exponential density variation should apply. Also shown in Figure 11 is the theoretical $N(z)$ obtained from Equations (1) and (8). In computing the theoretical $N(z)$ from Equation (8), the $\rho(z)$ in the denominator of the term

$$\frac{g}{\rho(z)} \frac{d\rho(z)}{dz}$$

was approximated by a constant, $\rho(z_a)$. The error incurred by doing this is not significant, and greatly simplifies further theoretical development. With the above approximation, the theoretical $N^2(z)$, plotted on Figure 11 is:

$$N^2(z) = -\left\{ \left[ -\frac{g\Delta\rho}{\rho(z_a)\overline{\ell}_\rho} \operatorname{sech}^2 \frac{2}{\overline{\ell}_\rho}(z - z_a) \right] + g^2/c^2 \right\} \qquad (16)$$

In Figure 11 the theoretical curve has been adjusted to provide a good fit; the maximum stability frequency, $N_{max}$, is thus not exactly the same for both curves, the $N_{max}$ = constant portion of the experimental curve having a slightly lower $N_{max}$ than the theoretical curve.

The characteristic equations corresponding to the two types of density distributions are as follows. For the exponential density distribution,

$$k_e(z) = \frac{n\pi}{D} \frac{(\omega^2 - \Omega_f^2)^{\frac{1}{2}}}{(N^2_{max} - \omega^2)^{\frac{1}{2}}} \qquad (17)$$
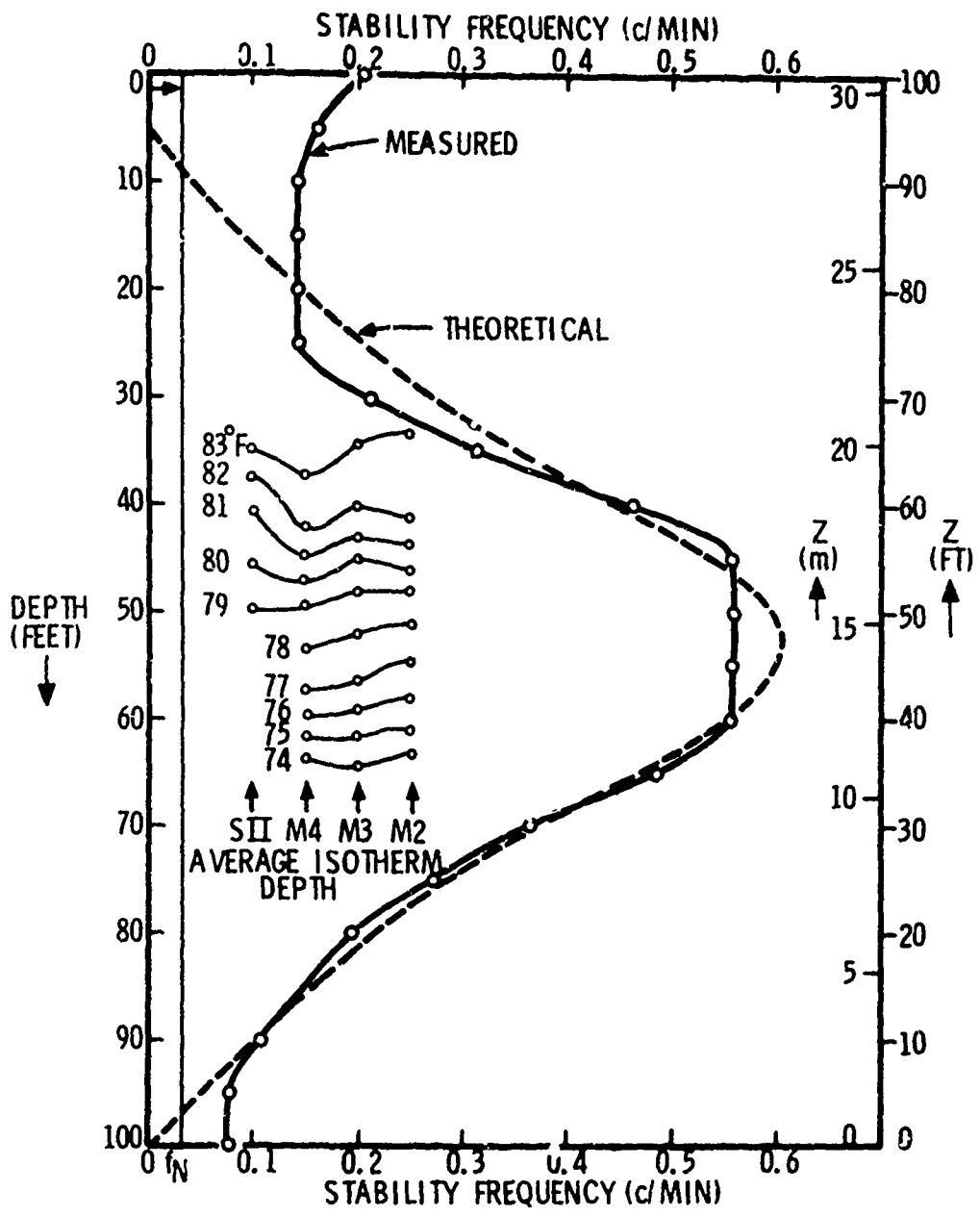
28

FIGURE 11. STABILITY FREQUENCY VERSUS DEPTH

where D is the total water depth, $\omega$ is the angular frequency of an internal wave whose corresponding wave number is $k_e(z)$, and $N_{max}$ is the stability frequency corresponding to the assumed exponential density distribution. Note that since $N_{max}$ is a constant value for all values of z, $k_e(z)$ is also the same for all values of z at any given frequency. The quantity n in Equation (16) is the mode number, i.e., the number of extrema of $\zeta(z)$ which occur if $\zeta(z)$ is plotted versus z. A first mode wave (n = 1) corresponds to the thermocline moving up and down as a whole; a second mode wave (n = 2) corresponds to the top of the thermocline moving up while the bottom moves down, causing an expansion and contraction of the thermocline, etc. Internal waves in general are thought to be linear combinations of several modes occurring simultaneously. In the work reported here, there was no evidence for waves other than n = 1 except at the internal tide frequency, for which there seems to be a combination of n = 1 and n = 2 waves. In what follows n = 1 is used throughout. The theory leading to Equation (17) has been worked out in the literature; both Eckart (Reference 25, p. 149) and Tolstoy (Reference 8) derive Equation (16). In Reference 25, Chapter 12, Eckart gives some general results for an N(z) of asymmetrical form and having one maximum.

The characteristic equation for the hyperbolic tangent density distribution (Equation 14) is

$$k_h(z - z_m) = \frac{n\pi}{D} \frac{(\omega^2 - \Omega_v^2)^{\frac{1}{2}}}{\left\{ \left[ N_{max}^2 \operatorname{sech}^2 \frac{2}{\ell_\rho} (z - z_m) \right] - \omega^2 \right\}^{\frac{1}{2}}} \qquad (18)$$

The relation between Equations (17) and (18) is clear; at $z = z_m$, $k_e = k_h$, and at depths away from the center of the thermocline, Equation (18) differs from Equation (17) by the presence of the $\operatorname{sech}^2$ factor in the denominator. Inspection of Equation (18) reveals an aspect of internal waves which is not demonstrated by the simpler exponential density case, and which may have important implications regarding propagation of internal waves in shallow water; this aspect has apparently not been previously pointed out in the literature explicitly. At any given frequency, the presence of the $\operatorname{sech}^2$ factor causes $k_h(z - z_m)$ to have a minimum at $z = z_m$, and increasing values for increasing $|z - z_m|$, i.e., the wave number at a given frequency is depth dependent. Since the wave phase velocity is the ratio of frequency to wave number, $\omega/k_h$, and since $k_h$ increases with the distance away from the center of the thermocline, it is seen that the phase velocity versus depth relation (at a given frequency) is analogous to a divergent sound channel for acoustic propagation, i.e., the phase velocity, $c_0$, has a maximum at the center of the thermocline, and decreases away from the center, according to the Equation

$$c_0(\omega,\ z - z_a) = \frac{\omega D}{n\pi}\ \frac{\left\{\left[N^2_{max}\ \text{sech}^2\ \frac{2}{l_0}\ (z - z_t)\right] - \omega^2\right\}^{\frac{1}{2}}}{(\omega^2 - \Omega^2_t)^{\frac{1}{2}}} \qquad (19)$$

This effect is shown in Figure 12 where Equation (17) (and Equation (18) for $z = z_a = 47$ feet) is plotted as the upper curve (labeled Depth 53 feet). Aslo shown are curves for distances of 16 and 32 feet (4.9 and 9.8 m) above and below the thermocline, computed from Equation (18). Such curves are known as diagnostic diagrams. A phase velocity versus depth relation such as predicted from Equation (18) has two immediate implications. The first is that if plane, first mode internal waves were generated over a substantial depth range and allowed to run free, all waves except those at the thermocline center would be refracted upward or downward, thus diverging the wave energy. Theoretically, such waves would be either reflected at the surface and bottom or refractively "turned" at some depth, so that the internal wave energy is "trapped" as in a wave guide. In the real case of shallow water, however, the upper and lower portions of the water column are well mixed, implying the presence of turbulence and other mixing processes. It is probable that internal waves refracted upward and downward into such turbulent regions would be destroyed by mixing in the sense that such waves would become noncoherent before being reflected back into the wave channel. Thus, under the stated conditions, the divergent nature of the thermocline region, combined with mixing above and below, may aid in accounting for the universally observed but unexplained fact that internal wave coherences are much lower (over distances of even less than a wavelength) than would be reasonably expected.

The second implication results from the fact that since internal waves at different depths have different phase velocities and wavelengths, one must be careful in performing averaging and other statistical operations over depth. However, waves at different depths and/or different locations, but at the same frequency, should be coherent in the statistical sense, since they are recorded as two time series of the same frequency but with different phases.

Turning again to the diagnostic diagram, shown in Figure 12, there are several features worth noting. Free internal waves of oscillatory type can exist only in the frequency range $\Omega_t < \omega < N_{max}$, due to the restriction in Equations (9) and (11) that $\gamma^2 > 0$. As $\omega \to \Omega_t$, $k(z) \to 0$ and $\lambda \to \infty$, indicating the resonance with which the local internal tides are associated. For frequencies less than about $10^{-3}$ cycles per minute, wavelengths are so large that assumptions underlying the theory are not met and consequently the theory as presented here is not valid. For frequencies greater than about $2 \times 10^{-3}$ cycles per minute the theory should be quite good. At the other end of the frequency range,
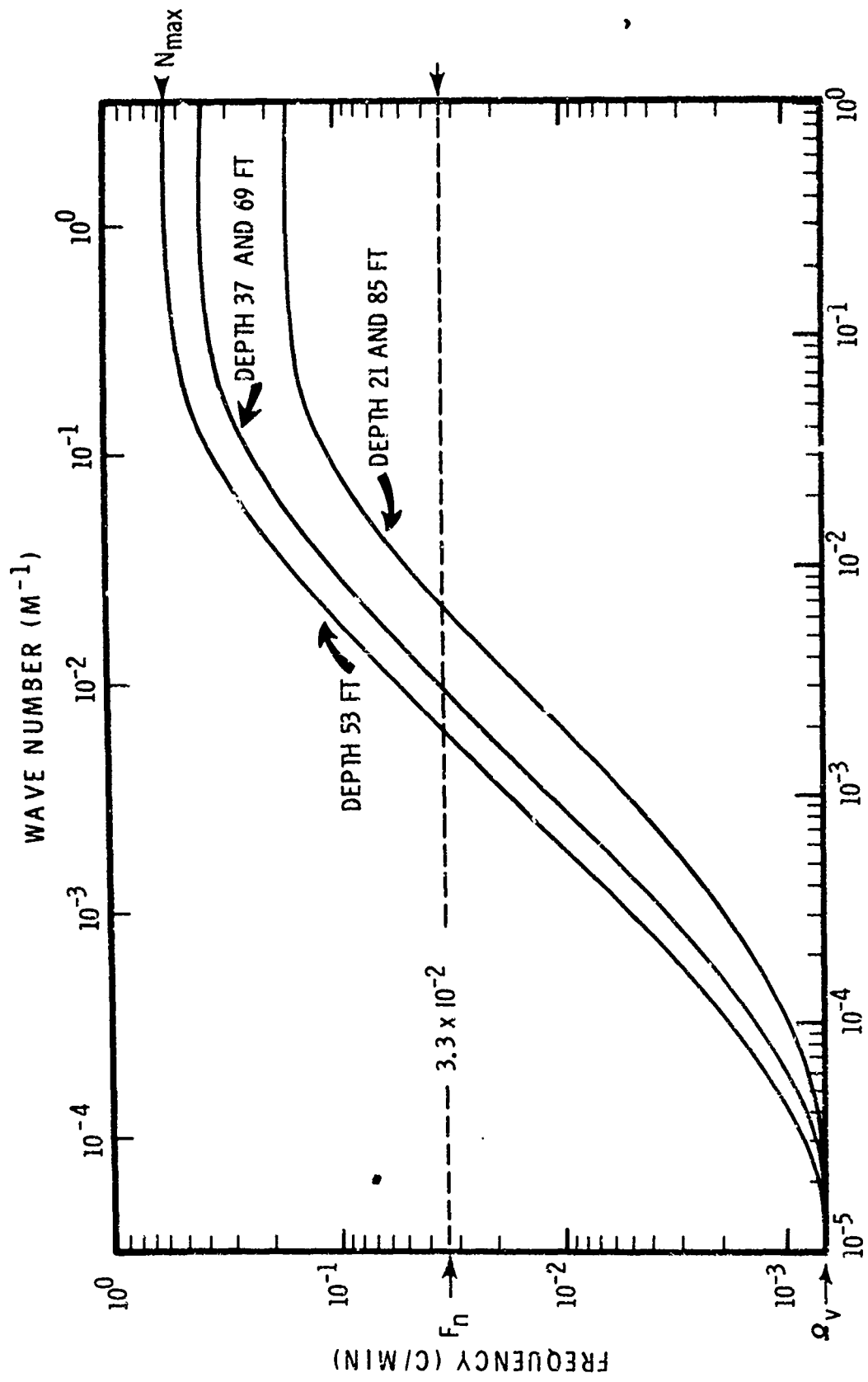
FIGURE 12. THEORETICAL WAVE NUMBER VERSUS
FREQUENCY - WATER DEPTH 100 FEET

32

as $\omega \rightarrow N_{max}$, $k(z) \rightarrow \infty$ and $\lambda \rightarrow 0$, corresponding to purely vertical "bobbing" motion.

Since the water depths involved in the survey were between 50 and 100 feet (15 and 30 m), over most of the frequency range the internal waves were "shallow water waves," i.e., their speed is controlled by water depth. This is shown in Figure 12 by the essentially linear portions of the curves; in this range, $d\omega/dk = 0$, and the group velocity is the same as the phase velocity.

Finally, note that in Figure 12 the Nyquist frequency $F_n$, is indicated as a broken line. Data resulting from the survey can yield information only for frequencies lower than $F_n$, corresponding to wavelengths of the order of $2 \times 10^3$ to $2 \times 10^4$ feet (6.1 to 61 km).

We now turn to the cross power spectra to obtain experimental frequency versus wavelength data to compare with theory

Figures 13 through 20 show typical examples of the many spectra that were computed. Note that the frequency scale ranges from zero to 0.033 cycles per minute; the $10^{-1}$ factor on the scale label should be interpreted as meaning "multiply any number on the frequency scale by $10^{-1}$."

Some comments on general features and shape of the spectra are in order. The most noticeable features are the large energy peak at the low frequency end of the spectrum, the monotonic decrease in energy down to levels at or slightly above the BT noise level, and the lack of any significant peaks. In general, the shape and energy levels of all the spectra are much the same, except for a weak indication that spectra of isotherms in the thermocline center have progressively lower energy levels in the offshore direction. All spectra have the same general form as that observed in spectra of turbulent flow. In order to see if the spectra follow a power law, all spectra were plotted on log power versus log frequency scales. Over approximately half the frequency range, all log-log spectra could reasonably be approximated by straight lines, indicating a relationship of the form

$$P(f) = c_1 f^{-m} + c_2 \tag{20}$$

where $P(f)$ is spectral power level at frequency $f$; $m$, $c_1$, and $c_2$ are constants. From the theory of homogenous isotropic turbulence (Reference 26), one would expect $m = 5/3$. Thirty-five estimates of $m$ measured from the spectra yielded a range of $m$ from 1.5 to 2.9, with an average of $m = 2.3$. There were weak trends indicating that $m$ is larger for nearshore stations and that $m$ is somewhat smaller for isotherms near the thermocline center; however, these trends were not
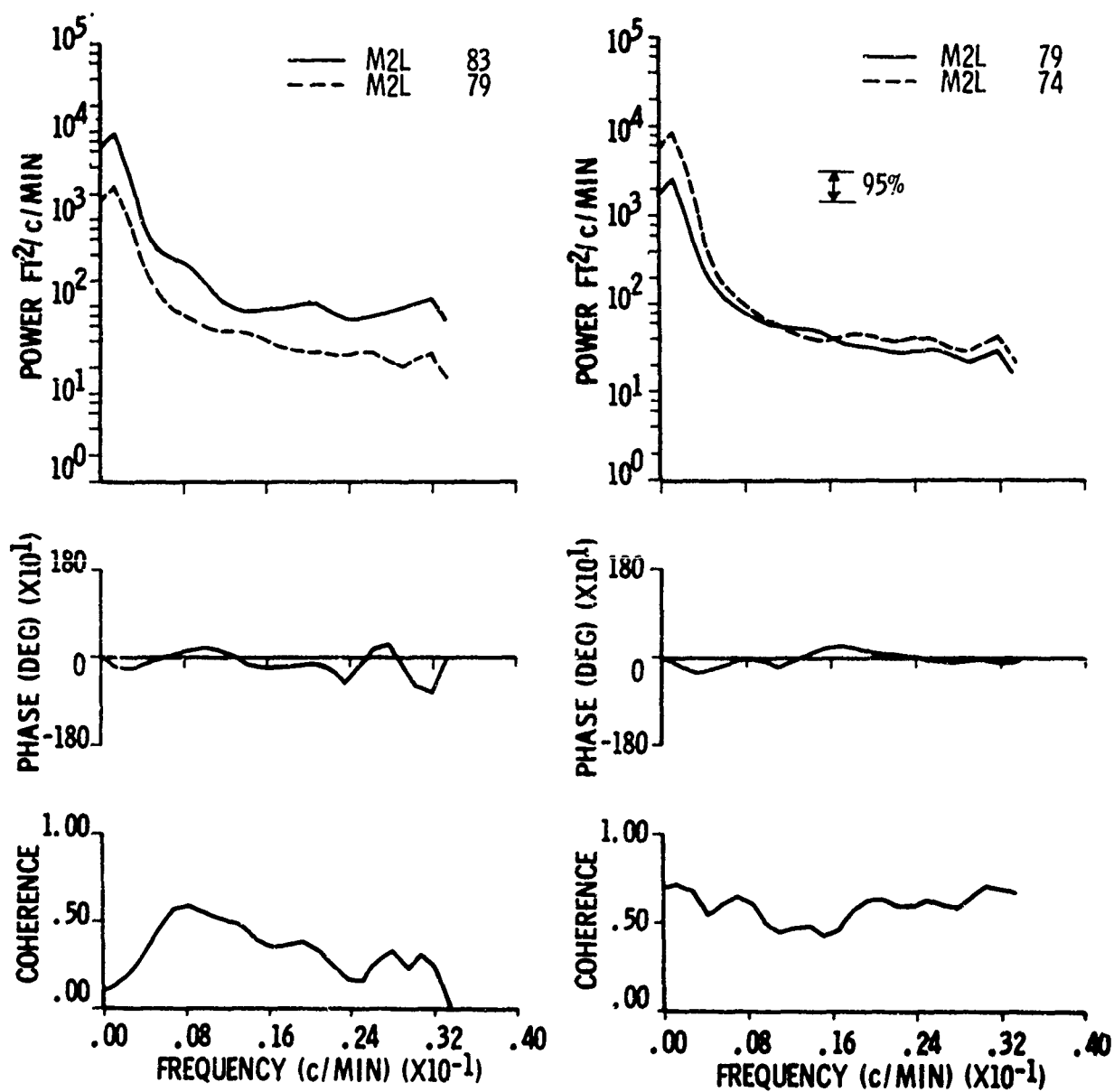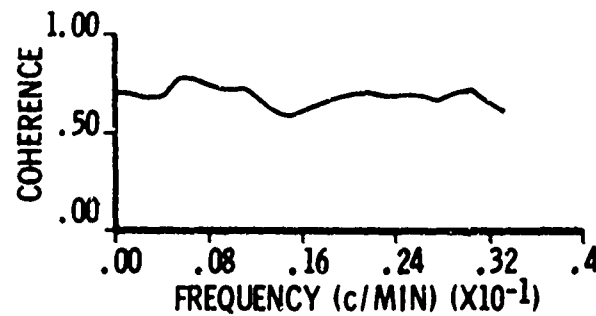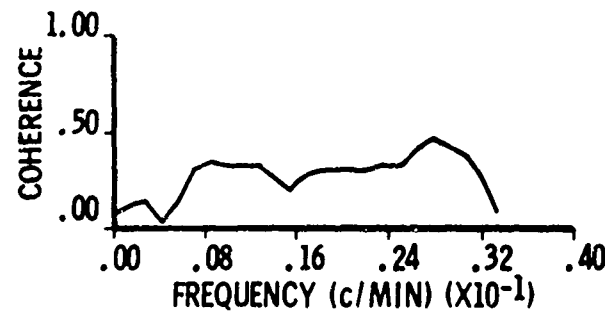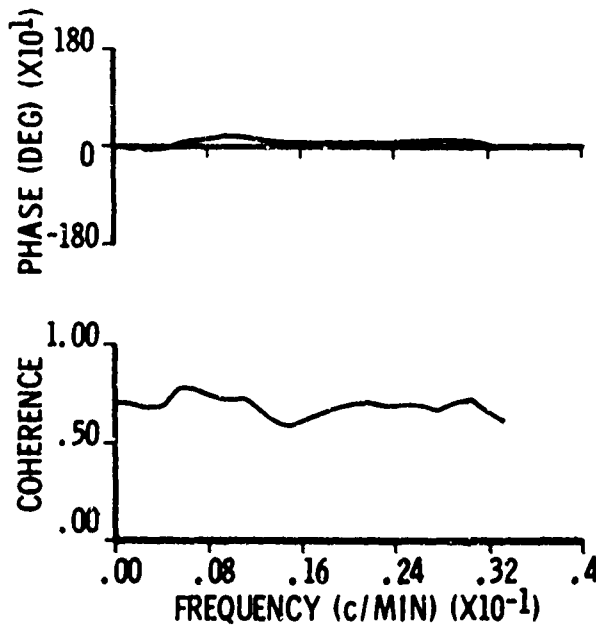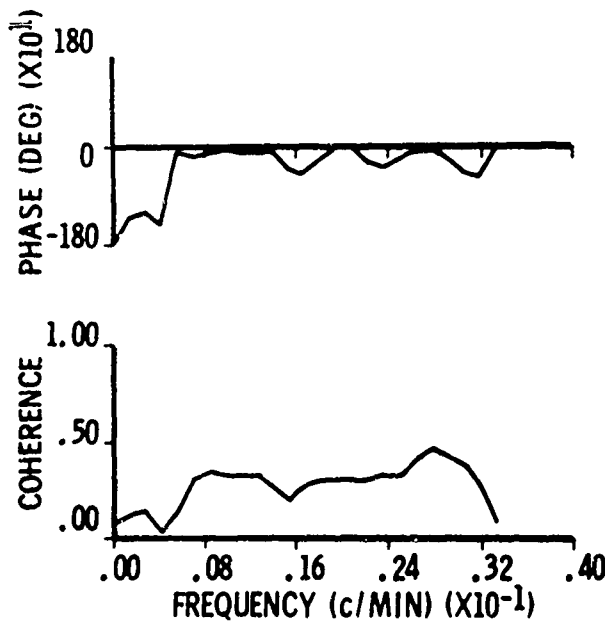
33

FIGURE 13. ISOTHERM POWER SPECTRUMS
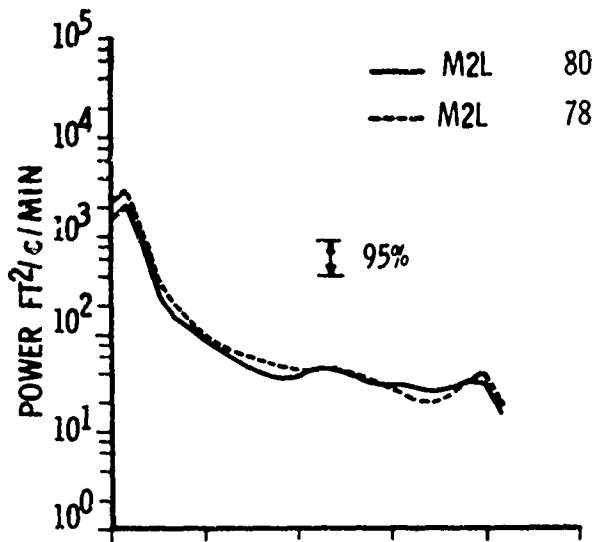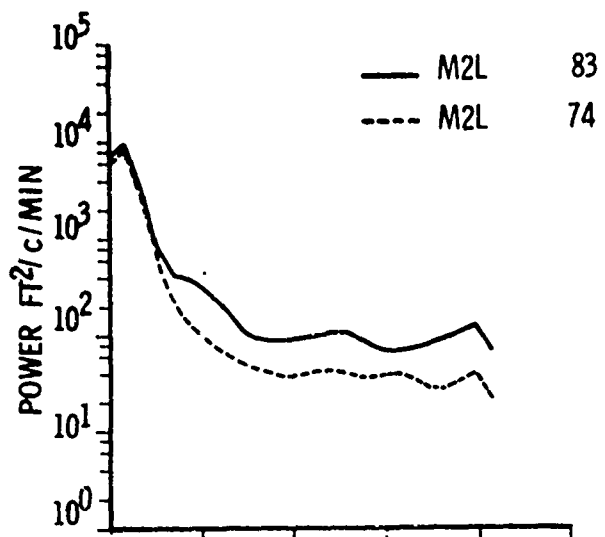
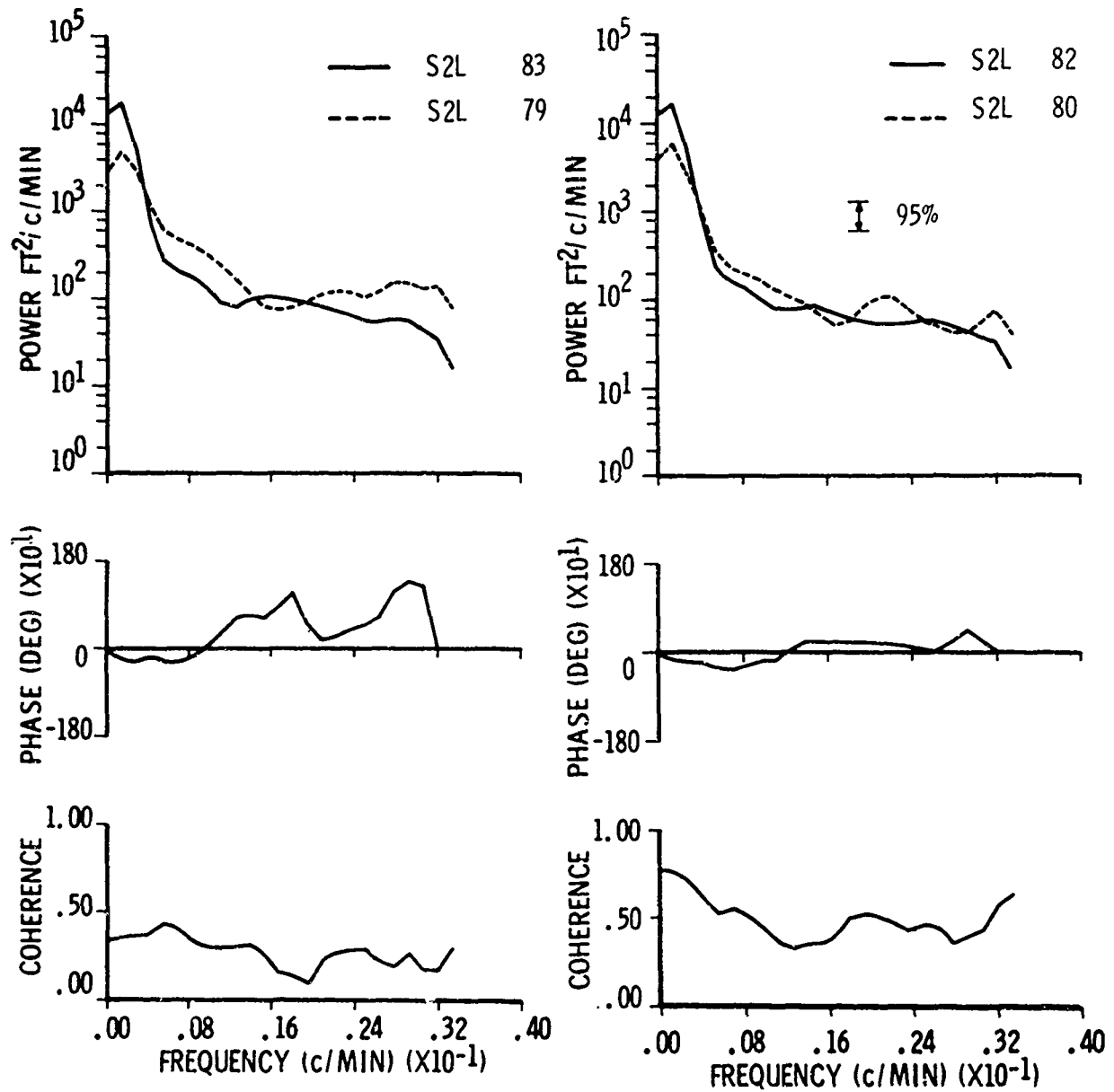FIGURE 14. ISOTHERM POWER SPECTRUMS

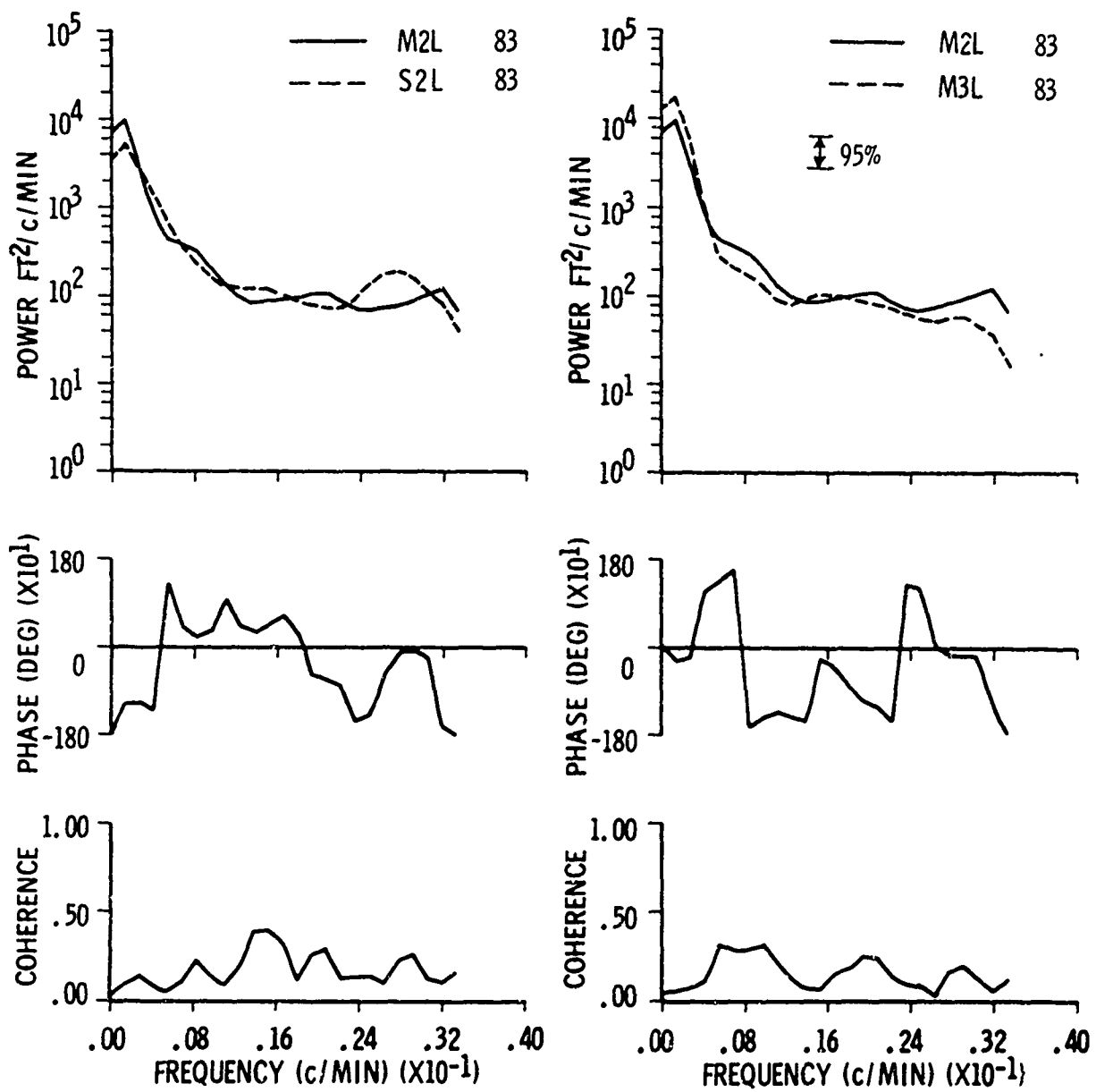FIGURE 15. ISOTHERM POWER SPECTRUMS
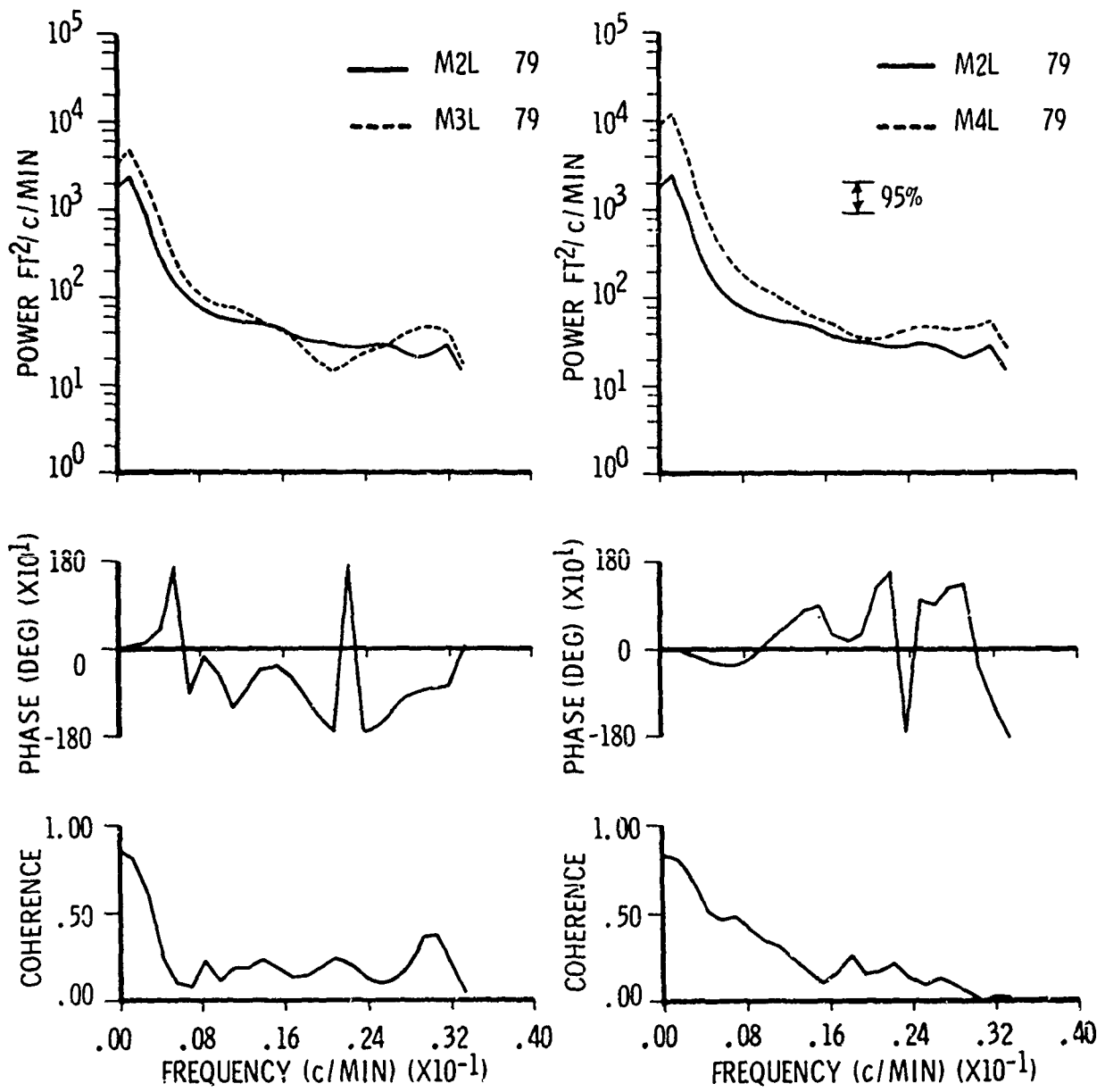
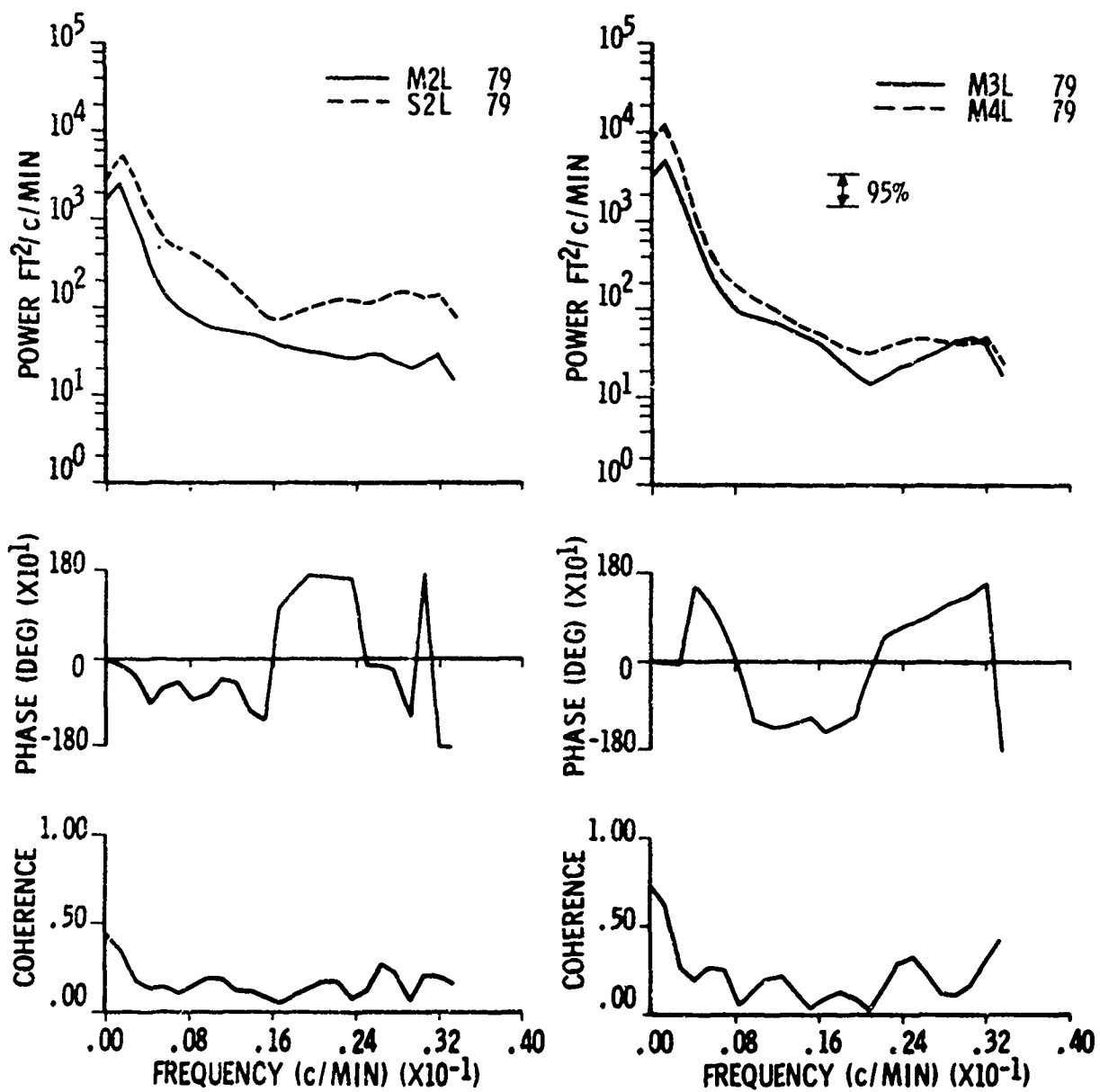FIGURE 16. ISOTHERM POWER SPECTRUMS

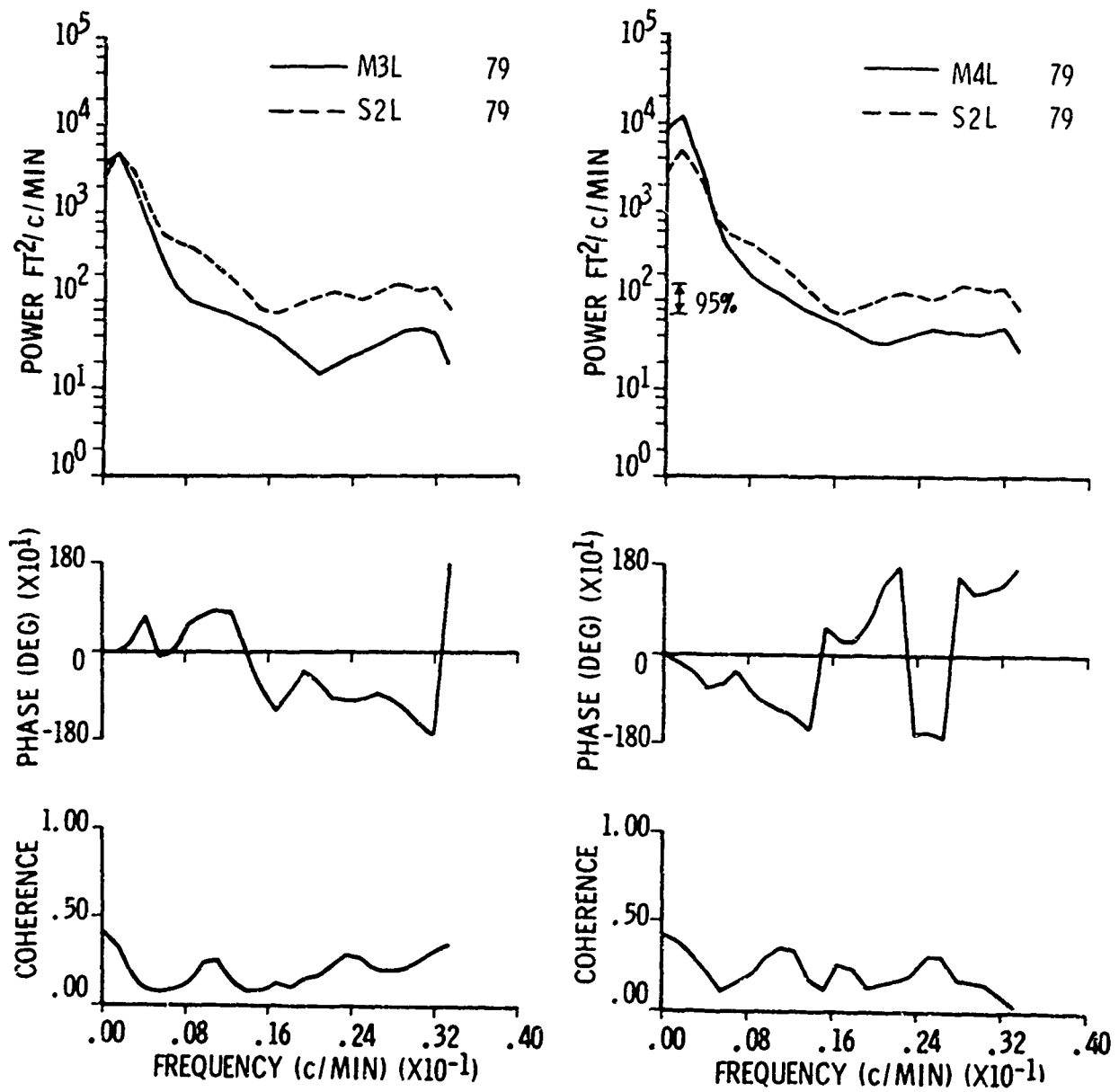FIGURE 17. ISOTHERM POWER SPECTRUMS

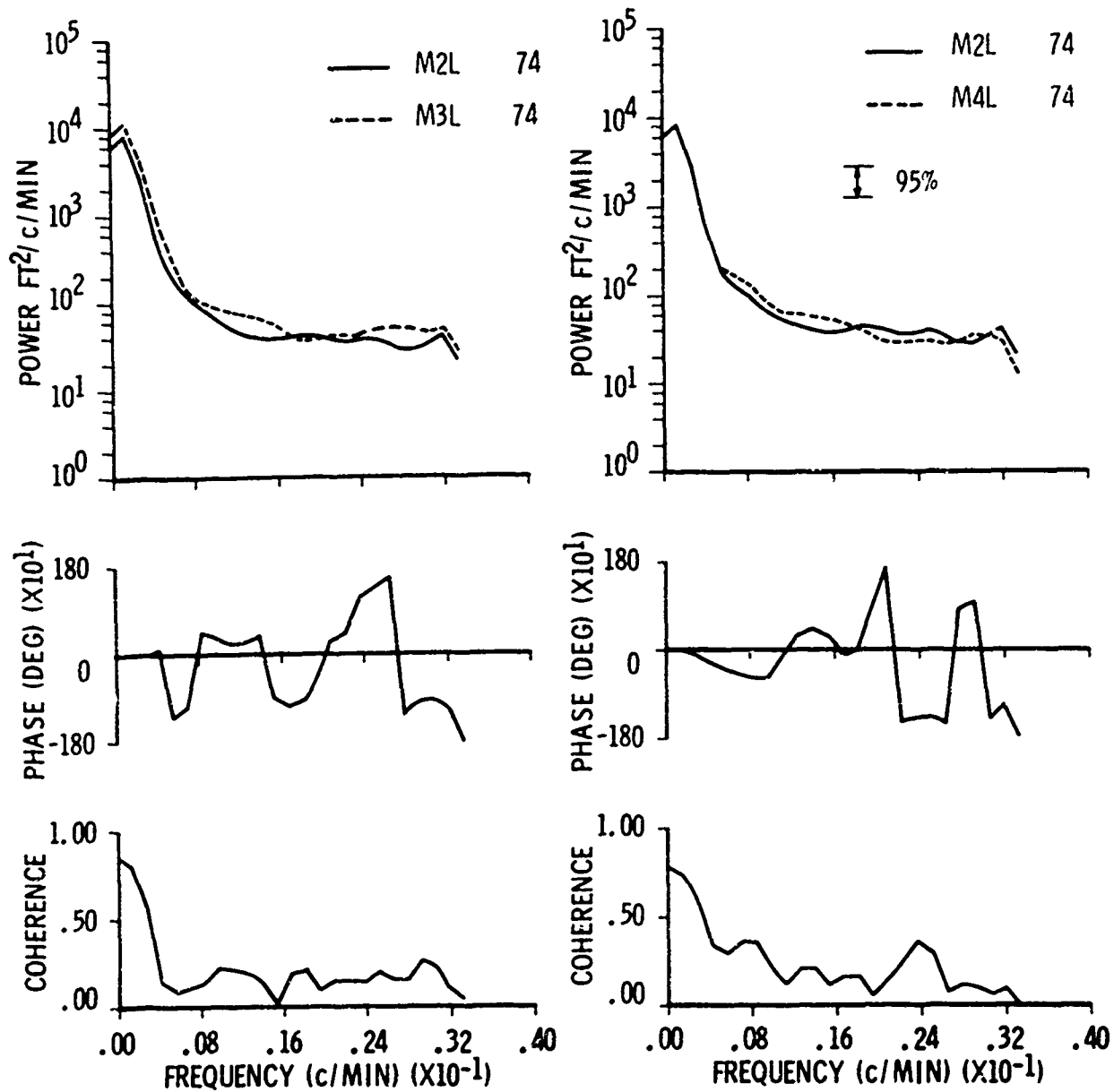FIGURE 18. ISOTHERM POWER SPECTRUMS

FIGURE 19. ISOTHERM POWER SPECTRUMS

FIGURE 20. ISOTHERM POWER SPECTRUMS

significant. The average m = 2.3 corresponds closely to m = 11/5 = 2.2, and is significantly different from m = 5/3. To account for m = 2.3 instead of m = 5/3, it is postulated that results presented here constitute a partial verification of a theory of turbulence spectra in stably stratified media developed by Bolgiano (References 27 and 28). In this theory, values of negative power law exponents larger than 5/3 are explained by modification of turbulent spectra due to the effects of buoyancy (gravity) forces resulting from stable stratification. The basis for this theory is that stratification is accompanied by anisotropy which reflects the uniqueness of the vertical direction. Under these conditions the equilibrium spectrum may be divided into three subranges: (1) the buoyancy subrange, associated with larger, anisotropic eddies directly influenced by the density stratification, (2) the inertial subrange in which the anisotrophy has been destroyed and the usual universal equilibrium theory (Reference 26), which predicts m = 5/3, is applicable, and (3) the dissipation subrange at high wave numbers where molecular effects dominate. Under these circumstances spectra for the buoyancy subrange are predicted to be proportional to $k^{-11/5}$, agreeing with spectra observed in this report. Unfortunately, adequate data are not available to calculate the theoretically predicted transition wave number $k_B$ which separates the buoyancy subrange from the inertial subrange; because of this, results presented here only partially verify Bolgiano's theory. Another result of Bolgiano's theory is in qualitative agreement with the previous discussion of the·observed equilibrium density distribution. This is that any mass transport, such as associated with turbulence, must be accompanied by a compensating influx and efflux of heat at the top and bottom surfaces of the stable water column. The energy abstracted from the turbulence is expended to transport heat vertically downward through the stratified medium, thus maintaining an equilibrium average thermal and density structure in spite of mixing.

Figures 13, 14, and 15 show cross-spectra resulting from crossing different isotherms within given stations. For both stations shown, there is no significant phase change between isotherms, indicating a first mode oscillation. Coherence between isotherms decreases with isotherm separation and is higher for isotherm pairs in the lower water layer than in the upper layer. Isotherms within either layer (e.g., M279 x M274 and M279 x M283), are generally more coherent than isotherm pairs in different layers (e.g., M283 x M274), indicating that there is independent generation of turbulence in the upper and lower water layers; this turbulence acts as incoherent noise added to wave motions present, causing a lowering of coherence. Note that in all cases the uppermost isotherm (83°F) is incoherent with either the center isotherm (79°F), the bottom isotherm (74°F), or isotherms at other stations; this is especially so at low frequencies where one would expect high coherence for long wavelengths. It is not generally possible to separate effects of turbulence by using spectra from a single location, because apparent

vertical isotherm motion can be caused by either wave motion or the passage of "frozen in" turbulent eddies being transported by a quasi-steady current. In order to look for internal wave effects we turn to cross-spectra of the same isotherms at different stations, examples of which are shown in Figures 16 through 20. If such spectra were obtained from internal wave motions only, they should be highly coherent for separations of one wavelength or less. On the other hand, if the spectra resulted only from independent, randomly generated turbulence at each station, the coherence should be nearly zero (except possibly for eddy sizes larger than several times the station separation). In the real case, it is likely that both effects are present, with the turbulence degrading the coherence due to internal waves. Note that for all pairs (except for Figure 16, involving the 83°F isotherm, which seems to be incoherent with everything) the coherence is generally highest at low frequencies (long wavelengths) and decreases with station separation. The phase spectra are related to the ratio of wavelength to interstation distance at each frequency; it is this relation that is used to derive experimental data to compare with the theoretical characteristic equation. Because the coherencies are generally low, causing instability of the phase spectra, averaging was done over the 75°F through 81°F isotherm cross-spectra for each station pair. This gave an effective increase in degrees of freedom, with a correspondingly better phase stability and lowered 95° confidence level for coherence. The technique used to determine experimental wavelength versus frequency relations from the spectra was as follows. It was assumed that for the long wavelengths involved any free internal waves would have been refracted before reaching the survey area so that all waves (within range of experimental measurement) would be coming from directly offshore, i.e., along the station line. This assumption is supported by both available observations (Reference 2) and theory. The next consideration is that if an internal wave has a wavelength equal to the distance between a pair of stations, then the phase separation is $2\pi$ (or, what is the same, zero phase shift); hence the phase spectra should be zero at the corresponding frequency. Likewise, if there are exactly two wavelengths between two stations, the phase spectrum should show a second zero at a higher frequency, etc.

Applying this technique to the averaged cross-spectra for all station pairs, there resulted 19 sets of frequency - wavelength data for which the coherence was higher than the 95 percent confidence level for coherence, i.e., the probability is less than .05 that these data resulted from uncorrelated random data. It should be pointed out that even the averaged data produced coherencies which were only marginally above the 95 percent confidence level, which was R = 0.15. The maximum averaged coherence was R = 0.49, and about half of the 19 sets of data had coherencies greater than 0.20. In spite of this coherence reduction by turbulent "noise" in the time series, there is the clear implication that the data show (with probability greater than .95) an experimentally

observed relationship between frequency and wavelength. If this
relationship agrees with that predicted from theory, and if no other
theoretical mechanism can be found to predict the same relationship,
we conclude that internal waves were present during the period of the
field survey. A comparison of experimental and theoretical data is
shown in Figure 21, in which the theoretical frequency-wavenumber
relation (from Figure 12) has been converted to frequency versus wave-
length for the water depths at each end of the experimental station line.
It is seen that there is good agreement between experiment and theory.
The theoretical curves are for the maximum wavelengths, corresponding
to the center of the thermocline. The experimental data points gener-
ally fall between the curves as would be expected. It is concluded
that the theoretical characteristic equation has been verified by the
experimental data.

There remains the possibility that the data points of Figure 21
could have been generated by the passage of "frozen in" thermal tur-
bulence transported by an average current. Using the assumption of
"frozen in" turbulence, thermal eddies of scale size L would be trans-
ported past a point by an average current V causing an apparent thermal
fluctuation frequency, f, according to the relation

$$V = fL, \text{ or, } f = VL^{-1} \tag{21}$$

On a log-log plot this equation has the form

$$\log f = \log V + (-1) \log L; \tag{22}$$

thus the slope of this function on a log-log plot is -1.

Likewise, in the range of frequencies

$$\Omega_v << \omega << N,$$

Equation (17) can be approximated by

$$k = \frac{2\pi}{\lambda} \equiv \frac{n\pi}{D} \frac{\omega}{N} \tag{23}$$

which leads, on a log-log plot, to an equation of the same form as
Equation (22)

$$\log f = \log \left(\frac{DN}{n}\right) + (-1) \log \lambda \tag{24}$$

Thus it is seen that it is possible to produce data from turbulent effects
which have the same slope of log f versus log $\lambda$ as the slope predicted
from internal wave theory. However, it is possible to distinguish between
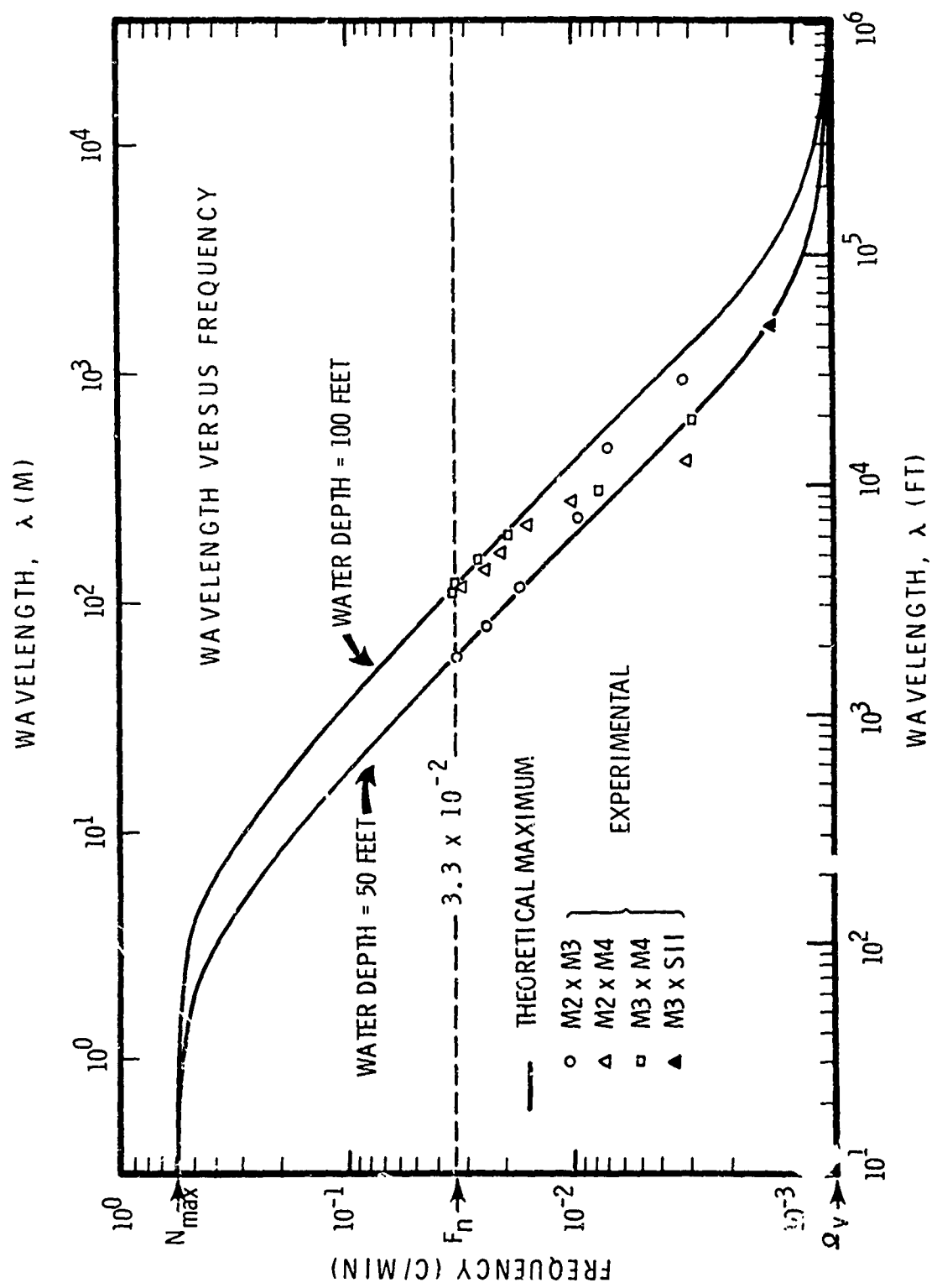
FIGURE 21. WAVELENGTH VERSUS FREQUENCY

these two cases on the basis of the average velocity that is required
to produce data (with a slope of -1) having the proper numerical values
of frequency versus wavelength as shown in Figure 21. From Figure 21,
it is seen that (since the curves are nearly linear over the range for
which we have data) in order to obtain such data using Equation (21),
the average current V must be about

$$V = 110 \text{ ft/min} = 1.1 \text{ knot} = 55 \text{ cm/sec} \quad .$$

The maximum current speed observed during the survey at station M3 was
1.0 knots (51 cm/sec) in the surface layer; from the same data the best
estimate of average current speed in the thermocline region is 0.4 knots
(21 cm/sec). Also, since the current exhibited large shears, with
larger speeds in the surface layer (average speed in surface layer was
0.6 knot (31 cm/sec) and in bottom layer was 0.14 knot (7 cm/sec)) than
in the bottom layer, there would be expected in the cross-spectral data
an observable change with depth of the frequency versus wavelength rela-
tion if it were caused by turbulence. Such an effect was not observable.
Thus, it is concluded that, with the possible exception of one point at
$f = 3.1 \times 10^{-3}$ cycles per minute, the data points in Figure 21 resulted
from passage of free internal waves whose characteristic equation,
derived from the measured density distribution, is Equation (16). Also,
because of the low coherencies observed between stations, and due to
the shape of the power spectra, it is concluded that the energy of the
internal waves (except for the internal tide) was small relative to the
energy of the turbulent thermal fluctuation present. Thus, the observa-
tions presented here are consistent with the idea that shallow-water
internal waves and turbulence are interrelated.

Further evidence for the existence and amplitudes of internal waves
at frequencies above the Nyquist frequency for the BT data is shown in
Figure 22; these data also provide information to show that high fre-
quency aliasing was not detrimental to isotherm power spectra resulting
from the BT data. Shown in Figure 22 are spectra derived from data
taken by the Texas A & M automatic data collection system. One spectrum
is of temperature fluctuations at 48-foot (14.5 m) depth; the other is
of current direction fluctuations at the bottom (depth 95 feet (29 m)).
The data used to compute the spectra were 1/2-minute averages of data
sampled at 1-second intervals, extending over about 17 hours. The
Nyquist frequency is 1 cycle per minute; hence these spectra cover a
frequency range about 30 times as large as the BT isotherm spectra. It
is evident from Figure 22 that the temperature spectrum at the thermo-
cline center approaches, for high frequencies, a substantially constant
spectral level of about $10^{-1}$ $(°C)^2$ per cycle per minute. Conversion of
this spectral level to equivalent vertical isotherm variation (in terms
of the known temperature gradient) yields an equivalent wave amplitude
of about 1.6 feet (0.5 m), which is sufficiently low compared to the
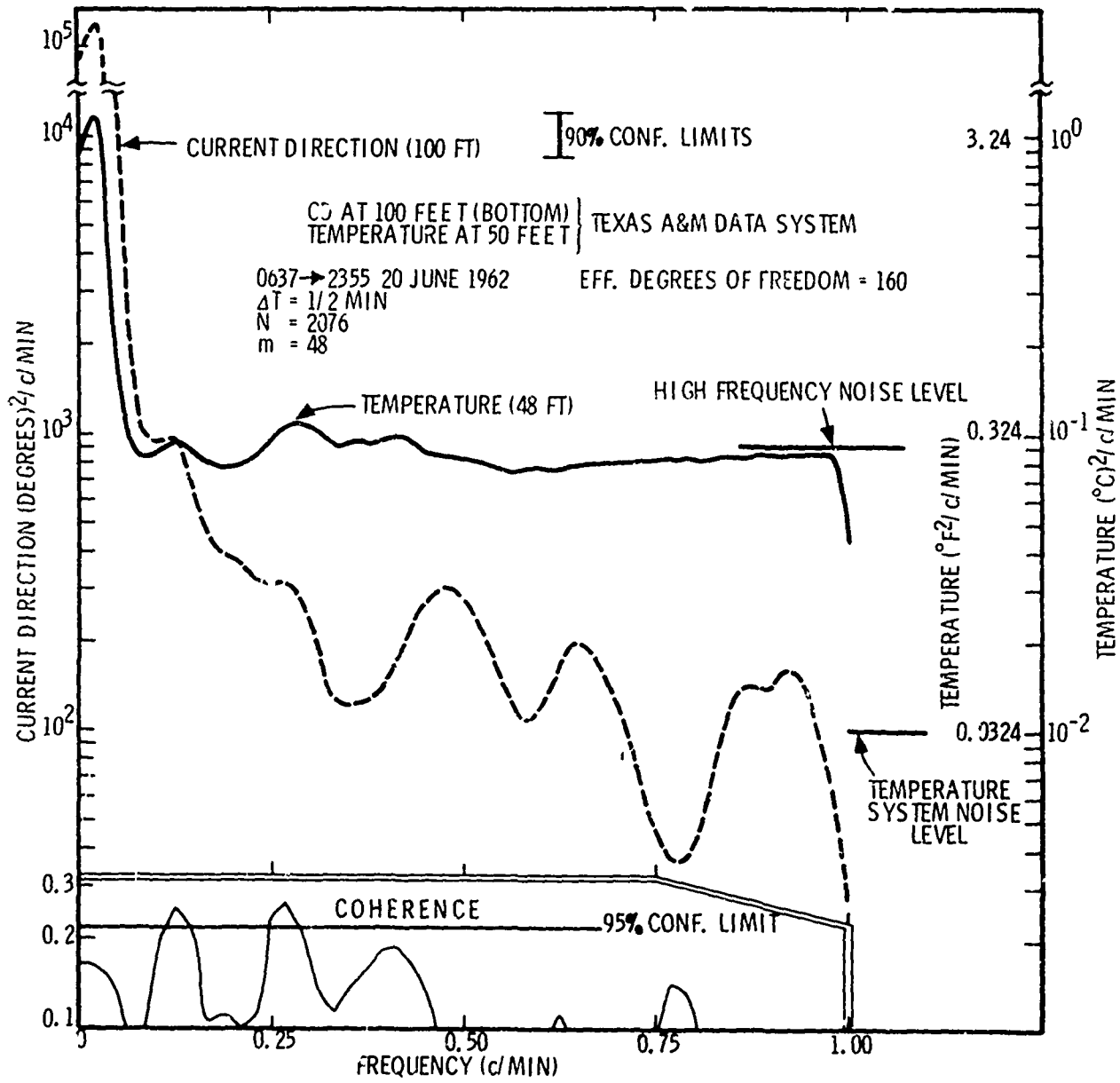
FIGURE 22. SPECTRUMS OF CURRENT DIRECTION
AND TEMPERATURE AT STAGE I

isotherm spectral noise levels (about 6 feet (1.8 m)) to insure that
aliasing effects, although not completely absent, were not of signifi-
cance for the analysis performed. Note that there are two "bumps" on
the temperature spectrum, at about 0.125 and 0.27 cycle per minute,
which, although discernible, are not significant. At these frequencies
the coherence between temperature at 48 feet (14.5 m) and current
direction at 95 feet (29 m) is above the 95 percent confidence level,
indicating a correlation between horizontal water motion at the bottom
and temperature variations at mid-depth. The only mechan' ¬ known to
the author which can account for this type of correlatior at these fre-
quencies involves shallow-water internal waves, i.e., waves whose
lengths are long compared to the water depth so that there is horizon-
tal wave-induced flow at the bottom due to wave motion in the thermo-
cline. Wavelengths for the two frequencies involved are about 1000
and 300 feet (300 and 90 m), respectively, in a total water depth of
100 feet (30 m), so that at these frequencies the waves are of the
shallow type.

An interesting feature was revealed by plotting the 1/2-minute
averages of current direction versus time. Over several sections of
the resulting record there were obvious wavelike variations of current
direction with periods in a range corresponding to the frequencies
observed above; in one section of the record about thirty such oscil-
lations were visible. These current direction oscillations apparently
result from a weak steady current in one direction being modulated by
internal wave-induced flow. Other sections of the record showed large
and irregular direction fluctuations with no discernible pattern; yet
other portions show weakly discernible wavelike fluctuations on which
are superimposed irregular fluctuations of random appearance. The
record could thus be described as being composed of alternating sections
of wavelike and random fluctuations. It is clear that a cross spectrum
resulting from two such records would have coherency reduced in pro-
portion to the percentage of random fluctuations in the records. It is
again concluded that the data indicate the presence of free internal
waves during the survey period. It is also suggested that use of cur-
rent direction fluctuations and their spectra may be a valuable but
neglected way to gain insight into ocean flow mechanisms. The usefulness
of wind direction spectra in understanding atmospheric flows has been
pointed out by Cramer (Reference 29).


## SHEAR FLOW AND TURBULENCE


As pointed out in the introduction and in the section on internal
tides, there exists a shear flow at the frequency of the internal tides
which might be expected to interact with internal waves of higher

frequency to produce turbulence. Although no complete theory is
available to account for such interaction, a simplified two-layer
model can be used to point out significant features.

For a stable two-layer system of finite depth with the lower
layer stationary, and with the upper layer moving at constant speed U
(and neglecting interfacial tension effects) it is known experimentally
(Reference 9) that for certain ranges of U interfacial waves sponta-
neously form and that at larger values of U these waves become unstable
and are destroyed by mixing. It has been shown theoretically
(References 30 and 31) that for such a model the phase speed of the
wave on the interface is, to a good approximation,

$$c = \frac{\omega}{k} = \frac{U}{2} \pm \left[ C_0^2 - \left(\frac{U}{2}\right)^2 \right]^{\frac{1}{2}} \tag{25}$$

where $C_0$ is the phase speed at the same frequency in the absence of
currents, i.e., the phase speed predicted by the characteristic
equation. In order that the phase speed be real it is necessary that

$$C_0^2 - \left(\frac{U}{2}\right)^2 > 0 \tag{26}$$

otherwise the phase velocity has an imaginary part, in which case the
wave is unstable. If the density distribution is continuous, instead of
two-layered, then $C_0$ is a function of frequency, $C_0(f)$, and may be
approximated over a substantial range of frequencies (from Equation (17))
by

$$C_0^2 = \frac{\omega^2}{k^2} \equiv \left(\frac{D}{n\pi}\right)^2 \left(- \frac{g}{\rho}\frac{d\rho}{dz} - \frac{g^2}{c^2}\right) . \tag{27}$$

Substituting Equation (27) in (26) yields (keeping in mind that for
stable stratification $d\rho/dz$ is negative, and is numerically greater
than $g^2/c^2$, so that

$$- \frac{g}{\rho}\frac{d\rho}{dz} - \frac{g^2}{c^2} > 0),$$

$$\left[ \left(\frac{D}{n\pi}\right)^2 \left(- \frac{g}{\rho}\frac{d\rho}{dz} - \frac{g^2}{c^2}\right) - \left(\frac{U}{2}\right)^2 \right] > 0 . \tag{28}$$

Equation (28) illustrates the fundamental physical principle that velocity
shear tends to destabilize waves, in opposition to the stabilizing effect
of stable density stratification. For the stable two-layer system being

considered in this section, the equation corresponding to Equation (28) becomes

$$\frac{g}{2k} \frac{\Delta\rho}{\rho} - (\frac{U}{2})^2 > 0 \qquad (29)$$

where $\Delta\rho > 0$ is the density difference between layers. For this case it is obvious that for any finite $U > 0$, there is a k sufficiently small, and a corresponding frequency, $f_u$, sufficiently large, that Equation (29) is not satisfied, and all waves with frequency $f > f_u$ will be destroyed by the instability. The physical effect is analogous to the case of ocean surface waves having their peaks sheared off by a following wind of velocity greater than the wave speed. If a broad spectrum of waves are present, destruction of waves of frequency $f > f_u$ results in mixing, which in a real two-layer model means that the sharp interface between layers is changed into a continuous density gradient. In turn, this density gradient causes a lowering of $C_0$, making $f_u$ smaller, which promotes mixing for lower frequency waves, causing a further thickening of the mixed layer, etc. In the mixing processes it would be expected that turbulence will be generated, which would cause a further interaction, due to abstraction of energy from the mean flow U, which could cause a decrease in U, thus closing the inter-action cycle on itself. It is clear that such a closed-cycle inter-action process is very complicated; however, one would intuitively expect that in such a situation there will be an eventual equilibrium between stabilizing and destabilizing forces, leading to an equilibrium density gradient.

In order to assess the effects of shear flows in the survey data, the net current shear vector, i.e., the vector difference between cur-rent vectors measured at 5 and 95-foot (1.5 and 29 m) depths, were computed from current meter data at station M3, and is shown in Figure 4. The magnitude of the current shear vector is shown as a function of time in Figure 23. There is no apparent regularity, or relation to either the surface or internal tides. It is clear that there was always a cur-rent shear of at least 0.3 knots (15 cm/sec). The average shear speed was $U_{AV} = 0.7$ knots (36 cm/sec), and the maximum was $U_{max} = 1.0$ knot (51 cm/sec). In order to use these values of $U_{AV}$ and $U_{max}$ in Equation (26), account must be taken of the dependence of $C_0$ on frequency. Figure 24 (which is Figure 21, transformed by the relation $C_0(f) = f\lambda$) shows this dependence. The constancy of $C_0(f) = C_s = 112$ feet per minute (57 cm/sec) over a relatively wide range of frequencies is characteristic of shallow-water waves. The vertical arrows in Figure 24 indicate the frequencies which, according to Equation (26), are associ-ated with instabilities caused by the average and maximum shear current. Observe that the instability frequency corresponding to the average shear current is very close to N, the measured maximum frequency possible
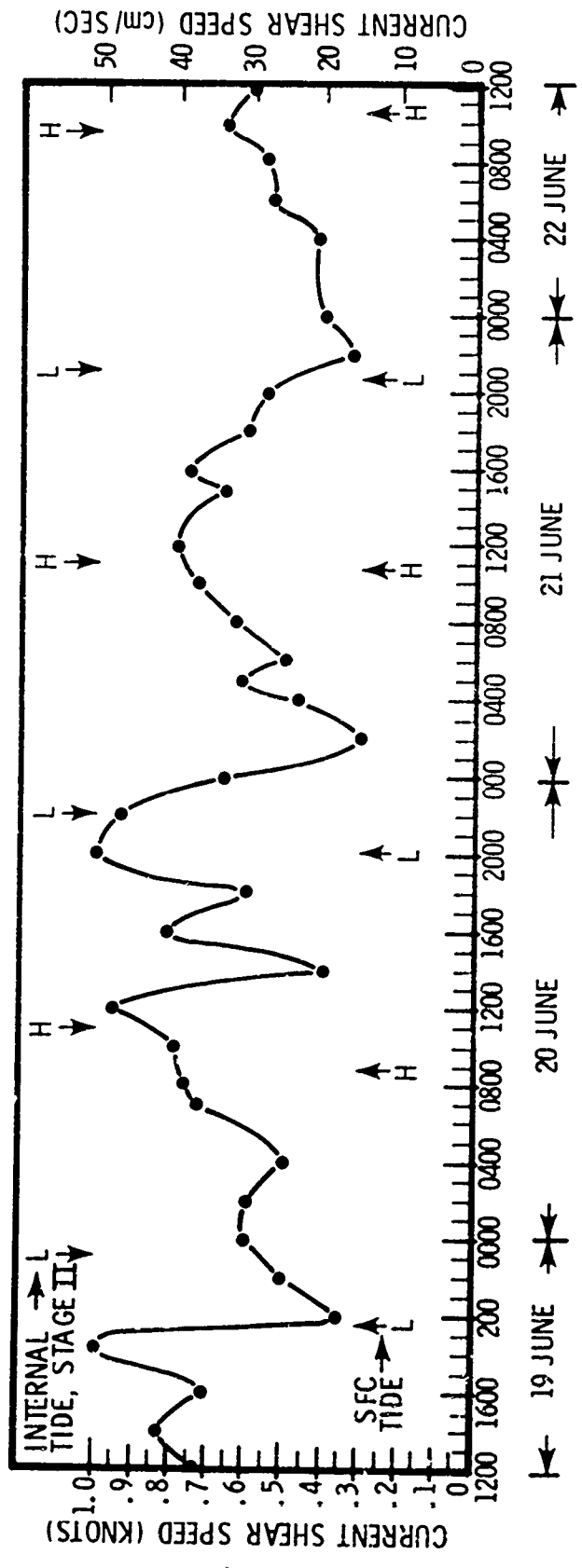
FIGURE 23. MAGNITUDE OF CURRENT SHEAR VECTOR
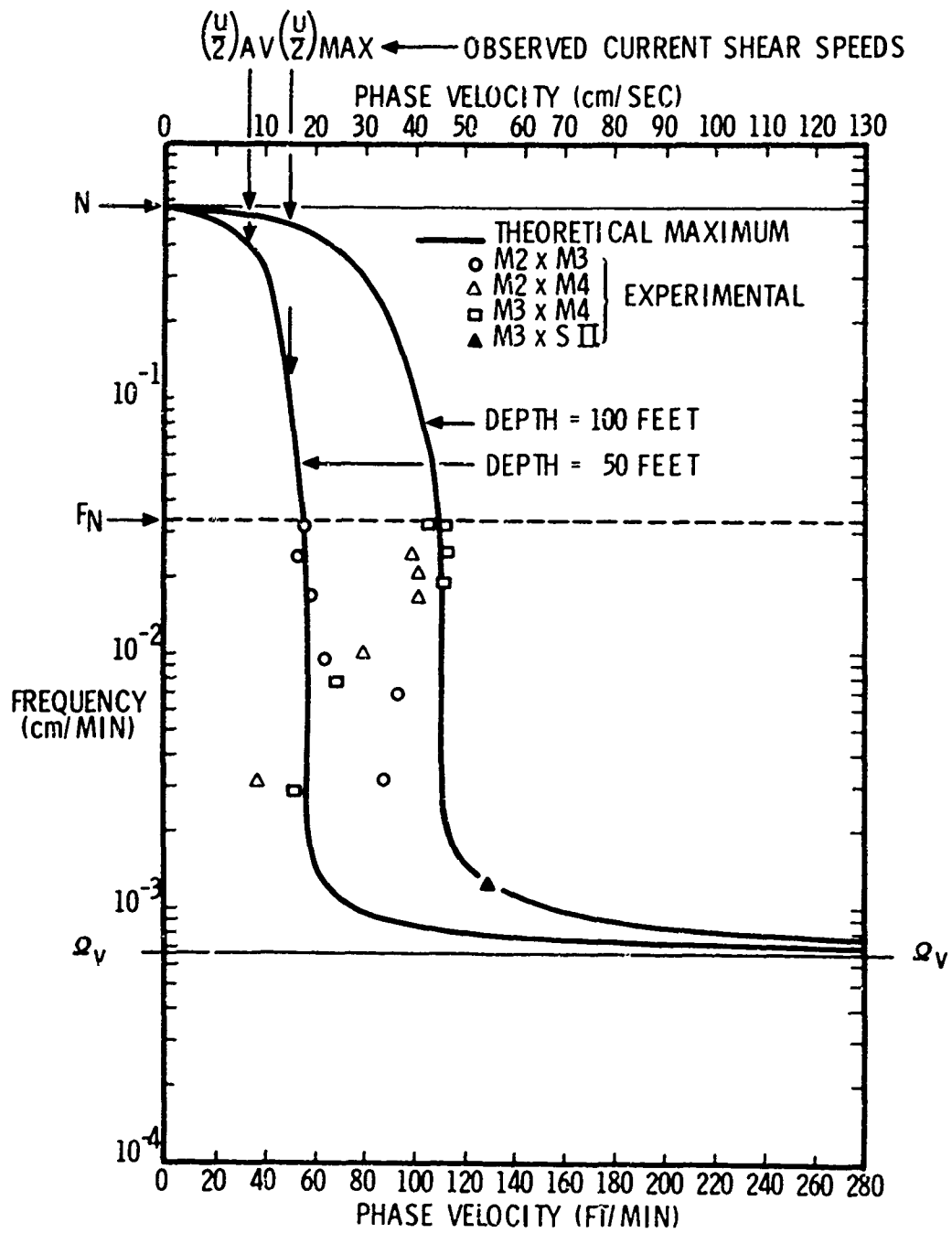VERSUS TIME, STATION M3

51

FIGURE 24. PHASE VELOCITY VERSUS FREQUENCY

for internal waves. Since, by Equation (26), on the average all waves of frequency higher than $C_0(f) = U_{AV}/2$ would be destroyed, with resulting modification of the density gradient, the observed closeness of $C_0(f) = U_{AV}/2$ to N is taken as experimental evidence that the previously described interaction between shear currents, waves and turbulence does indeed affect if not control the equilibrium density structure.

Note also that $U_{max}/2$ is about one half of $C_0(f) = C_s$ for the portion of the curve with nearly constant phase velocity. The curve for $C_0(f)$ represents maximum average stability at the center of the thermocline. Since in reality the stability varies in time (by a factor of two or more) it is likely that for short periods, $U_{max}/2$ may be close to $C_s$, causing turbulence at lower frequencies. However, it would be expected that $U_{max}/2$ would never exceed $C_s$, for if it did, the entire density structure would be destroyed; a stable density structure was always present during the field survey.

Another criterion which gives information about the existence of turbulence in a shear flow is the Richardson number,

$$R_i = \frac{-\dfrac{g}{\rho}\dfrac{d\rho}{dz}}{\left(\dfrac{du}{dz}\right)^2}$$

which is the ratio of density stabilizing forces to shear flow destabilizing forces. If $d\rho/dz$ is large and $du/dz$ very small, then $R_i$ is large, the flow is stable, and turbulence is suppressed. If $d\rho/dz$ is small and $du/dz$ large, then $R_i$ is small and any turbulence present will be maintained. Note that this criterion does not predict whether or not turbulence will actually be present, but only that turbulence, once generated, will be either suppressed or maintained. The critical value of the Richardson number above which turbulence will be suppressed and below which it will be maintained is generally accepted (References 30 and 32) to be approximately

$$R_i \text{ (crit)} \equiv 0.25 \quad .$$

Calculations of $R_i$ were made from the experimental data, using a value for $g/\rho \, d\rho/dz$ corresponding to the maximum stability at the thermocline center. Since the velocity gradient $du/dz$ was not measured in detail, two assumptions were used: that the observed velocity difference between surface and bottom was either (a) linear over the water depth, or (b) linear over the mixing layer thickness, $\ell_D$. The actual velocity distribution was probably somewhere between these two assumptions. The results were, for case (a) $0.24 \leq R_i \text{ (crit)} \leq 2.3$, with an average of 0.6; for case (b), $0.03 \leq R_i \text{ (crit)} \leq 0.3$, with an average of 0.1. It is thus apparent that on either assumption the observed Richardson numbers were

in the proper range for turbulence to be present at least part of the time.

It is concluded that experimental data support the concept that in shallow water, shear flows, internal waves and turbulence mutually interact to produce an equilibrium density gradient and that through such an interaction, internal waves will always be accompanied by simultaneous turbulence. It is also concluded that the results given here represent an observation of interaction between different parts of an internal wave spectrum, in that shear flows due to low-frequency (internal tide) waves affect waves at higher frequencies.

## SUMMARY

From cross-spectral analysis it has been concluded that free, low-frequency, internal waves were present during a three-day survey at Panama City, Florida. The data were contaminated by incoherent noise due to turbulence. Data were found to satisfy the characteristic equation from internal wave theory. Other evidence is significant coherence between thermal fluctuations at mid-depth and current direction fluctuations at the bottom, implying shallow-water internal waves.

Internal wave theory has been extended to discussion of the case in which the density varies as the hyperbolic tangent with depth, a representation found to agree well with the observed average density distribution. Resulting from this is an analytical expression (Equation (19)) for variation of internal wave phase velocity with depth at any given frequency. This expression implies that shallow-water internal waves in such a density profile will be dissipated by divergence of wave energy into the upper and lower turbulently mixed layers, which are necessarily associated with this type density distribution. This effect may partially account for the observed low coherencies of internal waves.

Power spectra of observed isotherm fluctuations are shown to have a form agreeing with the theory of anisotropic turbulence. The observed spectra thus result from superposition of two classes of spectra, one (weaker) due to internal waves, and one (stronger) due to turbulence.

Theory and experimental data support: (1) the concept of mutual interaction of internal waves, shear flows, and turbulence, (2) the idea that these interactions determine the equilibrium density profile, (3) the conclusion that internal waves (at least in shallow water) will always be accompanied by turbulence, thus causing low coherencies in internal wave cross-spectra, and (4) the conclusion that the results

given here represent an observation of interaction of one part of an internal wave spectrum with another part.

For guidance of future research there is a need for a detailed quantitative theory to account adequately for the qualitative mutual interaction concepts described here. It is hoped that results presented in this report will be useful in development of such a theory. It is also hoped that these results will serve to emphasize the fact that internal waves and turbulence (in shallow water at least) cannot be treated as separate phenomena, especially in investigation of sound transmission through nonhomogenous oceans. In any in situ oceanic experiments, with stratification such as described here, there will be times when effects of internal waves predominate, and other times when turbulence effects predominate; means must be provided to measure and account for both phenomena.

There results, from the preceding conclusions, the following postulated qualitative dynamic model of the nearshore, shallow-water, summertime ocean at Panama City, Florida, which is consistent with observed data:

(1) There exist large amplitude, long wavelength, forced, internal tide waves which are associated with resonance between diurnal surface tides and motion in the inertia circle. These waves, at the low-frequency limit of the free internal wave spectrum, cause significant large-scale, quasi-steady shear flow between the upper and lower water layers associated with density stratification present during the summer.

(2) A continuous spectrum of free internal waves is generated over the permissible frequency range (as determined by the stability frequency) by various generation processes which as yet remain largely unknown in detail. Generation mechanisms thought to be responsible (but not directly proven in the open ocean) are (a) nonlinear interaction between surface waves and internal waves, (b) flow over an irregular bottom, (c) generation by shear flow (as in (1) above, for certain ranges of shear flow) and (d) generation by moving atmospheric pressure perturbations at the surface. Waves corresponding to the lower frequency, long wavelength part of the spectrum are in shallow water, and these waves are refracted shoreward. As they approach the shore these waves travel more slowly and their wavelengths shorten. The higher frequency, shorter wavelength part of the spectrum contains waves which travel very slowly.

(3) The current shears from (1) tend to destroy these slower moving waves in (2), producing turbulence and modifying the density gradient toward an equilibrium structure. Also, all waves except those traveling at the center of the thermocline will be diverged

upward or downward into the mixing zones in the upper and lower layers, leading to a degradation of internal wave energy. The result is that little of the higher frequency energy travels in the form of internal waves as far as the thermal shoreline; thus there is no turbulent internal wave surf.

(4) It appears that generation, amplification, and destruction of internal waves are in a steady state with respect to large-scale energy input through the sea surface and from earth rotation. The internal wave-shear flow-turbulence interactions can be thought of as part of the chain of physical processes which transport and convert energy from the solar system at large scales through smaller and smaller scales, ultimately resulting in molecular dissipation as heat.

and the crew of MSB-5, who, while operating virtually without rest for the whole period, willingly and with neither question nor complaint, performed feats of shiphandling without which the survey would have been crippled.

REFERENCES

1.  Rapports et Proces - Verbaux des Reunions, Conseil Permanent International Pour L' exploration de la Mer, Vol. LXXVI (1931).

2.  Lee, O. S., "Internal Waves in the Sea:  A Summary of Published Information with Notes on Application to Naval Operations, U. S. Navy Electronics Laboratory Report 1302 (26 July 1965).

3.  Iida, H. and Ichiye, T., "Edge Waves Over a Sloping Beach in a Rotating Two-Layered System," Technical Report 4 (April 1963), The Oceanographic Institute, Florida State University, Tallahassee, Florida (Unpublished Manuscript).

4.  Rattray, M., "On the Coastal Generation of Internal Tides," Tellus, Vol. 12, p. 54 (1960).

5.  Duxbury, A. C., "An Investigation of Stable Waves Along a Velocity Shear Boundary in a Two-Layer Sea with a Geostropic Flow Regime," Journal of Marine Research, Vol. 21, No. 3 (1963).

6.  Cox, C. and Sandstrom, H., "Coupling of Internal and Surface Waves in Water of Variable Depth," Journal of the Oceanographic Society of Japan, 20th Anniversary Volume (1962).

7.  Ball, F. R., "Energy Transfer Between External and Internal Gravity Waves," Journal Fluid Mechanics, Vol. 19, No. 3 (July 1964).

8.  Tolstoy, I., "The Theory of Waves in Stratified Fluids Including the Effects of Gravity and Rotation," Review of Modern Physics, Vol. 35, No. 1 (1963).

9.  Lofquist, K., "Flow and Stress Near an Interface Between Stratified Liquids," Physics of Fluids, Vol. 3, No. 2 (1960).

10. Ippen, A. T., and Harleman, D. R. F., "Steady State Characteristics of Subsurface Flow in Gravity Waves," National Bureau of Standards, Circular 521 (1952), p. 79.

11. Black, C. F., "The Turbulent Distribution of Temperature in the Ocean," Bissett-Berman Corporation Report MJO 1049 (ONR Contract Nonr 4967(00)) (December 1965).

12. Salsman, G. G., "A Note on Periodic Temperature Variations in the Gulf of Mexico Near Panama City, Florida," Synopsis of paper presented at Coastal and Shallow Water Research Conference, Tallahassee, Florida (October 1961) (Unpublished).

13. Ichiye, T., "Internal Waves over a Continental Shelf," Technical Report 3, The Oceanographic Institute, Florida State University, Tallahassee, Florida (1963) (Unpublished Manuscript).

14. Boston, N. E. J., "The Internal Tide off Panama City, Florida," M. S. Thesis, Agricultural and Mechanical College of Texas (June 1963).

15. Boston, N. E. J., "Observations of Tidal Periodic Internal Waves Over a Three-Day Period off Panama City, Florida," Texas A & M Reference 64-20T (31 August 1964).

16. Gaul, R. D., "Instrumentation and Data Handling System for Environmental Studies off Panama City, Florida," Texas A & M Reference 62-1T (1 February 1962).

17. Bennett, C. M., Pittman, E. P., and Austin, G. B., "A Data Processing System for Multiple Time Series Analysis of Ocean Wave Induced Bottom Pressure Fluctuations," 1st U. S. Navy Symposium on Military Oceanography, U. S. Naval Oceanographic Office (1964).

18. Parzen, E., "Mathematical Considerations in the Estimation of Spectra," Technometrics, Vol. 3, No. 2, pp. 167-190 (May 1961).

19. Munk, W. H., Snodgrass, F., and Tucker, M. J., "Spectra of Low Frequency Ocean Waves," Scripps Institution of Oceanography Bulletin SIO Vol. 7, No. 4, pp. 283-362 (1959).

20. Haubrich, R. A., "Earth Noise, 5 to 500 Millicycles Per Second, Part I," Journal Geophysical Research , Vol. 70, No. 6, pp. 1415-1427 (1965).

21. Dowling, G. B., Salsman, G. G., Gaul, R. D. and Boston, N. E. J., "On the Factors which Influence the Summer Thermal Structure of Shallow Water," presented at the 2nd Western National Meeting of the American Geophysical Union, Stanford University (December 27-29, 1962).

22. Biot, M. A., "The Influence of Initial Stress on E¹ stic Waves," Journal of Applied Physics, Vol. 11, p. 522 (1940).

23. Cunningham, W. J., "Introduction to Nonlinear Analysis," McGraw-Hill, New York (1958).

24. Eckart, C., "Internal Waves in the Ocean," Physics of Fluids, Vol. 4, No. 7, pp. 791-799 (1961).

25. Eckart, C., "Hydrodynamics of Oceans and Atmospheres," Pergamon Press, New York, p. 149 (1960).

26. Batchelor, G. K., "The Theory of Homogenous Turbulence," University Press, Cambridge, Mass., p. 197 (1953).

27. Bolgiano, R., Jr., "Turbulent Spectra On A Stably Stratified Atmosphere," Journal of Geophysical Research, Vol. 64, No. 12, pp. 2226-2229 (1959).

28. Bolgiano, R., Jr., "Structure of Turbulence in Stratified Media," Journal of Geophysical Research, Vol. 67, No. 8, pp. 3015-3023 (1962).

29. Cramer, H. E., "Atmospheric Diffusion," Symposium on Diffusion in Oceans and Fresh Waters, T. Ichiye, Editor, Lamont Geological Observatory (December 1965) p. 151 (abstract).

30. Yih, C. S., "Dynamics of Nonhomogenous Fluids," Macmillan Company, New York, N. Y. (1965).

31. Long, R. R., "The Motion of Fluids with Density Stratification," Journal of Geophysical Research, Vol. 64, No. 12, pp. 2151-2163 (1959).

32. Defant, A., "Physical Oceanography," Vol. I, Pergamon Press, New York, N. Y., p. 392 (1961).

| DOCUMENT CONTROL DATA - R & D | | |
|---|---|---|
| (Security classification of title, body of abstract and indexing annotation must be entered when the overall report is classified) | | |

**1. ORIGINATING ACTIVITY** *(Corporate author)*

U. S. Navy Mine Defense Laboratory
Panama City, Florida 32401

**2a. REPORT SECURITY CLASSIFICATION**
UNCLASSIFIED

**2b. GROUP**
--

**3. REPORT TITLE**

LOW FREQUENCY SHALLOW WATER INTERNAL WAVES AT PANAMA CITY, FLORIDA

**4. DESCRIPTIVE NOTES** *(Type of report and inclusive dates)*
Final

**5. AUTHOR(S)** *(First name, middle initial, last name)*

George B. Dowling

| **6. REPORT DATE** November 1966 | **7a. TOTAL NO. OF PAGES** 59 | **7b. NO. OF REFS** 32 |
|---|---|---|

**8a. CONTRACT OR GRANT NO.**

**b. PROJECT NO.**
Subproject ZF 011 01 01

**c.**
Task 11275-11

**d.**

**9a. ORIGINATOR'S REPORT NUMBER(S)**
313

**9b. OTHER REPORT NO(S)** *(Any other numbers that may be assigned this report)*

**10. DISTRIBUTION STATEMENT**

Distribution of this document is unlimited.

**11. SUPPLEMENTARY NOTES**

**12. SPONSORING MILITARY ACTIVITY**
Commander, Naval Ship Systems
Command (SHIPS 1622B) Navy Dept.
Washington, D. C. 20360

**13. ABSTRACT**

Internal waves were investigated in water depths of 60 to 100 feet (18 to 30 m) during the time of strong summer stratification, and in the presence of well-developed internal tides.

Cross-spectral analyses indicate that free, low-frequency, internal waves were present during the three-day survey, although the data were contaminated by incoherent noise due to turbulence. The data were found to satisfy the characteristic equation from internal wave theory. Other evidence is the significant coherence between thermal fluctuations at mid-depth and current direction fluctuations at the bottom, implying shallow-water internal waves.

The assumption that the density varies as the hyperbolic tangent with depth agrees well with the observed average density distribution and permits obtaining from internal wave theory an analytical expression for variation of internal wave phase velocity with depth at any given frequency. Shallow-water internal waves in such a density profile are dissipated divergence of wave energy into the upper and lower turbulently mixed layers, accounting in part for the observed low coherence of internal waves.

Power spectra of observed isotherm fluctuations have a form consistent with the theory of anisotropic turbulence. Observed spectra result from superposition of two classes of spectra, one (weaker) due to internal waves and one (stronger) due to turbulence.

Theory and experimental data support: (1, the concept of interaction of internal waves, shear flows, and turbulence, (2) the conjecture that these interactions determine the equilibrium density profile, (3) the conclusion that internal waves (at least in shallow water) are accompanied by turbulence, causing low coherencies in internal wave cross-spectra, and (4) the conclusion that the results given here represent an observation of the interaction of one part of an internal wave spectrum with another part.

| 14 KEY WORDS | LINK A | | LINK B | | LINK C | |
|---|---|---|---|---|---|---|
| | ROLE | WT | ROLE | WT | ROLE | WT |
| Internal waves | | | | | | |
| Internal tides | | | | | | |
| Turbulence | | | | | | |
| Thermal fluctuations of shallow water internal waves | | | | | | |
| Stratified fluids | | | | | | |
| Wave spectra | | | | | | |

ERRATA SHEET

MDL UNCLASSIFIED REPORT 313

6 October 1967

1.  Page 13, paragraph 2, line 8 should read:

"Ekman meters and current drogues.  At S1, the Texas A & M automatic"

2.  Page 14, Figure 5:  distance indicated by the brace oetween SII
    and M4 should be 5 MI.

3.  Page 22, paragraph 2, line 10 should read "(Reference 21)."

4.  Page 33, paragraph 2, line 5 should read:

"$\dfrac{d\omega}{dk}$ = constant"